Rotating Detonation Engine Performance Trends Analysis and Surrogate Model-Based Prediction

Michaela R. Hemming*, Nathan J. Hemming†, Dian R. Hill‡, and Kunning G. Xu§

The University of Alabama in Huntsville, Huntsville, AL, 35899

The objective of this work is to perform a data-driven analysis of current, open sourced literature on rotating detonation engine (RDE) hot fire data from around the world in order to visualize performances across different RDE sizes, nozzle designs, injector designs, and propellants. This work includes an analysis of chamber length impact on combustion efficiency, and then a machine learning approach is employed to predict behaviors of both global engine performance and detonation wave performance using existing, open source data on RDE hot fires. This prediction model is validated with existing data from the UAH WASP Engine hot fire campaign. The analysis of existing data has provided more evidence for some claims in literature on the effects of total mass flow rate and equivalence ratio on wave speeds. A look at chamber length has found that peak performance occurs around a RDE channel gap-to-length ratio of around 0.11 and 0.13 given existing data. The results of the prediction model show that the best predictions based on inputs of equivalence ratio, total mass flow rate, and the combustor gap-to-length ratio were for thrust and chamber pressure, but the predictions for wave number and wave speed are not accurate. The predictions for the UAH WASP Data show that chamber pressure and thrust can be predicted with relatively low error, while characteristic velocity and wave speed are greatly under predicting the actual performance.

I. Nomenclature

A_{ch}	=	channel cross-sectional area
A_{th}	=	throat cross-sectional area
$AFRL$	=	Air Force Research Laboratory
CJ	=	Chapman-Jouguet
C^*	=	characteristic velocity
D	=	engine chamber outer diameter
I_{sp}	=	specific impulse
$JAXA$	=	Japan Aerospace Exploration Agency
L	=	channel length
$\dot{m}_T$	=	total mass flow rate
$\dot{m}'$	=	mass flux
MAE	=	mean average error
$MSFC$	=	Marshall Space Flight Center
N	=	wave mode/number of waves
$NASA$	=	National Aeronautics and Space Administration
P_C	=	chamber pressure
q	=	mass flux
RDE	=	rotating detonation engine
$RMSE$	=	root mean squared error
T	=	thrust
UAH	=	The University of Alabama in Huntsville

---

*Graduate Research Assistant, Mechanical and Aerospace Engineering Department, and AIAA Student Member.

†PhD Student, Computer Science Department. 0000-0002-1920-6434

‡Research Engineer, Propulsion Research Center, AIAA Member.

§Associate Professor, Mechanical and Aerospace Engineering Department, AIAA Associate Fellow.

v_{CJ}	=	Chapman-Jouguet (theoretical) detonation wave velocity
v_{det}	=	detonation wave velocity
Δ	=	channel gap width
ϵ	=	nozzle restriction ratio
η	=	channel gap-to-length ratio
Φ	=	equivalence ratio

II. Introduction

ROTATING detonation engines are considered a promising propulsion device for space and hypersonic vehicle applications. Many research institutions have devoted resources to study these devices to use in place of, or along with, existing propulsion devices. The reason for the extensive research in full and sub-scale engines and fundamental detonation combustion experiments comes from the potential for overall pressure gain in the device. Total pressure gain involves an increase in stagnation pressure through gas expansion in a constrained heat release environment. These systems provide higher work extraction and therefore are more efficient than traditional, deflagration combustion engines. However, the research community has only seen pressure gain in idealized, premixed CFD models of RDEs. At this time, we have yet to realize pressure gain in experimental devices. Due to losses in systems and the chaotic nature of the combustion process, it is difficult to predict performance and optimize these engines for the detonation behavior itself. The goal of this work is to assist with identifying experimental gaps in literature, an analysis of chamber length impact on combustion efficiency, and predict behaviors of both global engine performance and detonation wave performance using existing, open source data on RDE hot fires.

Most of the current work on hot fire testing of RDEs is on smaller scale, low flow rate, heat sink devices. Additionally, there is a lack of consistency between the different engines resulting in too many variables to make adequate comparisons. For example, different research institutions will use different geometries, injectors, and/or propellants. This limits the range of possible performance behavior explored here. To accommodate somewhat for the variations, in this paper we only considered gaseous methane or hydrocarbons fuels. Also, most open source published results have very little repeatability efforts. This is most likely due to the costly and time-consuming nature of these experiments. However, in order to prove the validity of the results, it's necessary to repeat experiments. This paper later will discuss the implications of repeatability on prediction efforts. Another challenge of this comparison analysis and prediction effort is that much of the work on experimental RDEs are not open source given their potential applications in the space and defense industry.

Employing a prediction model will help establish a key step in the scientific method of establishing a concrete hypotheses to transition from exploratory based research on RDEs. Identifying where on the performance map the community has already studied and where we haven't looked at yet will help guide future research efforts. In a similar mindset to employing machine learning techniques to hot fire data, there have been research efforts with the Department of Energy to employ different neural network models for time series classification to determine real-time wave modes in RDE hot firings [1]. In another data driven, machine learning approach to understanding RDEs, the University of Washington has leveraged machine learning algorithms to overcome limitations imposed by RDE transnational invariance to combustion front dynamics [2]. All of this is done to construct a reduced order model to simulate the complex behavior of detonation waves. A similar survey of existing literature in order to guide design decisions for RDEs was conducted by the Combustion Devices group at NASA MSFC where the authors analyzed injector designs and their pros and cons for use in additively manufactured RDEs [3]. Pusan National University has published a literature survey on both pulse detonation engines as well as RDEs and discussed current research in a literature review approach that discussed key results of RDE research [4]. A similar literature review was performed by a group out of Peking University on RDE research progress [5]. Kriging methods like the one that is employed for this prediction model have been used for many prediction applications outside of experimental engine tests such as satellite data on air pollution [6], prediction of river channel topography [7], and diesel engine optimization [8], to name a few. The Kriging method is one of many methods that use sampled data to estimate values over a continuous spatial field in unsampled locations. It has many potential applications. This paper will explore how well this method can be applied to RDE hot fire data.

III. Methodology

This work was accomplished in two phases: a comprehensive survey and analysis of existing, open source RDE experimental data, and the construction and an accuracy review of a surrogate prediction model using Kriging models to

predict the performance of a newly hot-fired RDE at UAH.

A. Literature Survey and Trend Analysis

The literature survey consisted of data comparison from 6 different publications and research institutions and one internal test results that have not yet been published. This resulted in a total of 229 hot fire data points for this analysis. A summary of each test campaign's engine size, propellants, and injector is reported in Table 1 along with their respective citation.

Organization/Device	Engine Size	Propellant	Injector	Citation
UAH/Racetrack	4-inch ∅ 4-inch Linear	Propane-Oxygen Methane-Oxygen	Shear Coaxial	[9]
NASA MSFC	6.25-inch ∅	Methane-LOX	Triplet Pentad	[10]
Nagoya & JAXA	1.77-inch ∅	Ethylene-Oxygen	Slit Doublet Triplet	[11]
Purdue	3.7-inch ∅	H_2O_2-Triglyme	Triplet	[12]
AFRL	3-inch ∅	Methane-Oxygen	Doublets	[13]
Stechmann	3.88-inch ∅	Hydrogen-Oxygen Natural Gas - Oxygen Methane - Oxygen	Jet-in-Crossflow	[14]
UAH/WASP	3.05-inch ∅	Methane-Oxygen	Pentad	

Table 1   Summary of Surveyed RDE Test Campaigns

To collect the data necessary to make comparisons to existing experimental engine hot fire data, the authors began by creating a large repository of open source publications on RDE hot fire research. Each paper was reviewed in detail and a list of all available information the paper provided was created. This included geometry, injector type, propellants, test conditions, and how the authors of the original papers measured performance. Based on what was determined to be important information for this study compared to what was available, the necessary sub-calculations that can be made with the information provided in literature were identified. A list of they type of data in the final analysis is as follows:

- Nozzle Restriction Ratio
- Chamber Length
- Combustor Area
- Channel Gap
- **Channel Gap-to-Length Ratio**
- Equivalence Ratio
- Mass Flow Rate
- **Mass Flux**

- Detonation Wave Speed
- Number of Waves
- Chamber Pressure
- Thrust
- Specific Impulse
- **CJ Speed Ratio**
- **CJ Wave Speed**
- **Characteristic Velocity**

Data types in bold font are ones that were not provided by the original paper authors, but were calculated based on what was provided. While these are all the desired variables for this analysis, some papers did not report on some data. For example, the UAH Racetrack and work performed by NASA MSFC did not report on thrust. Also, the work by JAXA did not report on detonation wave activity. Therefore, these groups may not be included on some performance plots. However, some values can be predicted using ideal rocket relationships. Assuming an adiabatic flame temperature given the propellant mixture, exit pressure is equal to ambient pressure, and assuming constant ratio of specific heats, the thrust can be predicted for comparisons using the relationship shown in the equation below. Reported values for groups that are estimated are denoted in the legend with an astricks. Once the important parameters and variables have been decided, this will disqualify some of the papers due to insufficient or unclear information. Before down-selection, this work started with over 20 published RDE hot fire papers. A master spreadsheet of all provided data and sub calculations

was used to easily track and visualize the data. To obtain some of the numbers, a plot digitizer was necessary. This does mean that in papers that reported data in plots instead of tables, that the digitizer may not capture every repeated set point, especially when clustered. The tests that were considered repeat tests were used to determine the standard deviation of those data points. Since not all papers reported repeatability, a blanket standard deviation determined by other papers will be used for the prediction model. More will be discussed on this in the next section. The data was then batch-plotted to compare results including a look at how combustion chamber length impacts combustion efficiency. All of the data, except for the UAH WASP test campaign is then fed into the Kriging prediction model. The WASP data was not included because the prediction model will be validated with that data.

$$F = \dot{m}V_2 = \dot{m}\sqrt{(\frac{2\gamma}{\gamma - 1}RT_{ad})[1 - (\frac{p_2}{p_1})^{\frac{\gamma-1}{\gamma}}]} \tag{1}$$

There were some data points the authors wished to compare but couldn't because of the lack of repeated reported data types from different research institutions. For example, a look at all impinging injector types compared to coaxial types could provide insight into injector performance, but no two research institutions had the same type of injector. The same thing for nozzles. The only comparison we may be able to do is for straight channels, but no two organizations had the same nozzle restriction or expansion ratios.

B. Surrogate Model

A Kriging model [15] (also referred to as Gaussian Process) was chosen as the modeling method for predicting RDE characteristics. Kriging models were chosen because they work well with small to medium data sets, and the predictions produce a distribution instead of a single value. One can either sample the output or measure the confidence in the output with a corresponding mean value. Ideally Co-Kriging would be used, but the authors are unaware of any low fidelity model that captures the trends of RDE performance. Co-Kriging allows using a combination of low fidelity data with high fidelity data to improve overall model performance and reduce the number of high fidelity samples required.

The data for building the model was normalized between zero and one as this is common practice that yields better performing models. The reason for scaling the data between zero and one is to make each field have the same range. This is important to prevent one field dominating another. For example, wave speed can vary by thousands of feet per second, but equivalence ratio is all clustered around one. The order of magnitude difference can make wave speed dominate equivalence ratio. Equation 2 outlines the scheme to scale the data between a target values (min_{norm} and max_{norm}) using the minimum and maximum values of the range of the field. The performance of the model is measured with root mean squared error (RMSE) 3 and mean absolute error (MAE) 4.

$$x_{norm} = \frac{x - min}{max - min} * (max_{norm} - min_{norm}) + min_{norm} \tag{2}$$

$$RMSE = \sqrt{\frac{\sum_{i=1}^{N}(x_{i_{truth}} - x_{i_{pred}})^2}{N}} \tag{3}$$

$$MAE = \frac{1}{N}\sum_{i=1}^{N}|x_{i_{truth}} - x_{i_{pred}}| \tag{4}$$

The model was trained using 10 percent of the data for validation and 90 percent of the data for training. The data taken on the WASP engine was used as the testing data. N-fold cross validation with ten folds was used to measure the robustness of the model. N-fold cross validation is where random sub-sample of the data is used for validation and the remaining data is the training data. The constructed model measures its error over the validation data, then a new random sub-sample is taken from the original data set to be the new validation set. Again, the remaining data is the training data. This is repeated N times making n-folds. If the performance across the model is similar, the model is considered to be robust and the performance is not driven by a fortunate sub-sample. An RBF [16] [17] and a Matern kernel [17] were used for model. The hyper-parameters of the kernel function for the model were tuned by hand, minimizing the average root mean squared error (RMSE) over the n-folds. The results section contains the output of a model that was randomly selected from the cross validation study.

All of the code to create the models are available on github at `https://github.com/nhemming/RDRE_Injector_Modeling`. It does not require any python experience to run as it is set up to be input file based.

4

IV. Results

The results are divided into two sections: literature survey comparison and the prediction modeling. The first section will include the comparison plots generated with a description of what they are and why they were chosen. A discussion of the trends will also briefly be reported here and in more detail in the next section. The results of the Kriging prediction effort is also reported here. Further discussion on the implications and improvements of the results will be in the subsequent section.

A. Literature Survey

The first comparison made in Figure 1 was a map of the test conditions considered for each test point. The majority of the test points are at lower total mass flow rates except for the work by NASA MSFC and the dissertation published by Stechmann at Purdue University. A wide range of equivalence ratios appears to be tested with a majority of them being at rich conditions. Many research efforts have found that RDEs achieve the highest performance at an equivalence ratio of 1.1 for hydrocarbon fuels, more specifically for methane. A push for higher flow rates would give the community a better understanding of RDE performances. However, the lack of data at these flow rates could be because those test are not published in open source journals and conferences.
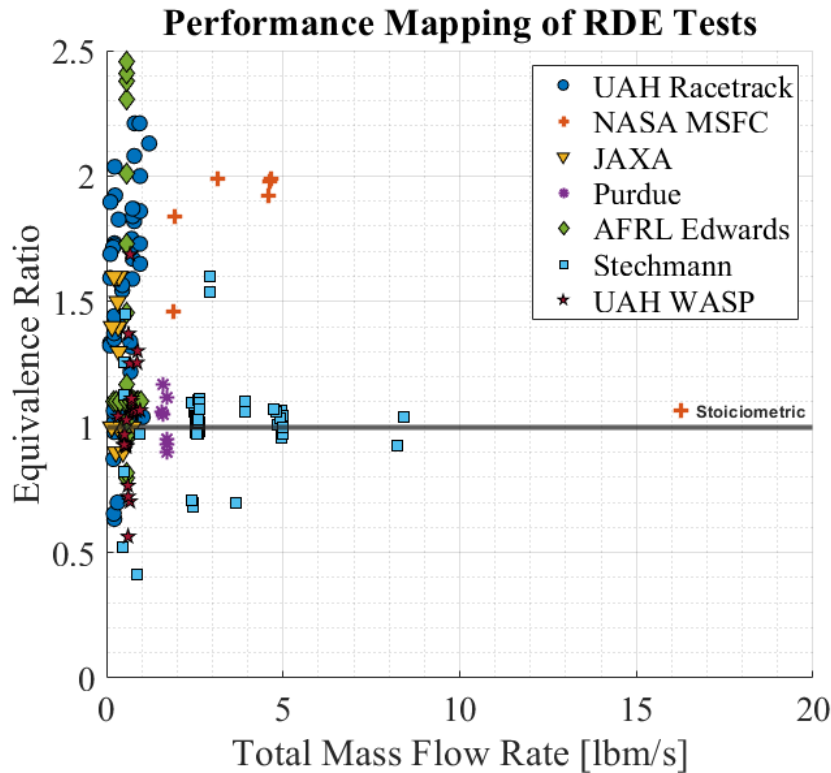
Fig. 1   Equivalence Ratio vs. Total Mass Flow Rate of Surveyed RDE Hot Fires

A comparison between test articles and their thrust output for a given total mass flow rate and mass flux is shown in Figure 2. Mass flux is calculated using the cross sectional area of the chamber rather than the flow areas of the injector as most papers do not report on injector flow area.

$$\dot{m}' = \frac{\dot{m}_T}{A_{ch}} \tag{5}$$

As expected, there is a linear trend between thrust and mass flow rate meaning that the higher the mass flow rate, the more thrust output. With the mass flux plot, there appears to be a deviation where there are two linear trends originating from the same intercept. This could be that the performance of the engine is impacted by the engine's geometry.

The left figure in Figure 3 considers the specific impulse performance of RDEs at different equivalence ratios. Specific impulse was chosen to effectively normalize the performance as opposed to comparing to thrust or chamber

5
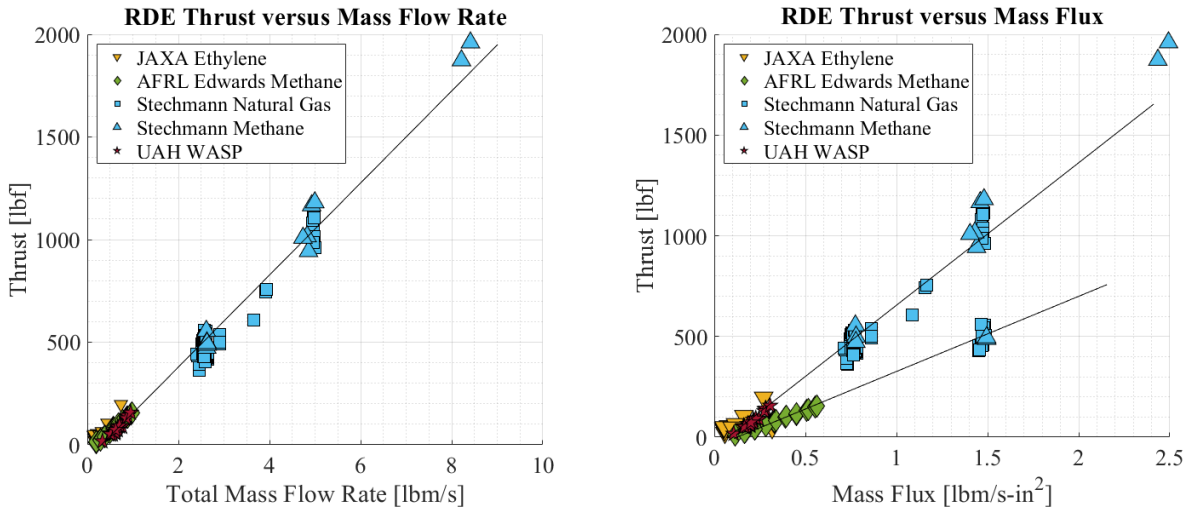
Fig. 2   Left: RDE Thrust vs. Total Mass Flow Rate | Right: RDE Thrust vs. Mass Flux

pressure. Unsurprisingly, the highest specific impulse output tends to occur around an equivalence ratio from 1.0 to 1.1, or around stoichiometric conditions. This makes sense because test conditions away from the ideal ratio of a mixture means that there is incomplete combustion of reactants in the chamber. The specific impulse of RDEs that were fired with hydrocarbon fuels was compared to the engine mass flux in the right figure in Figure 3. As mass flux increases, the specific impulse also increases until a mass flux of about 0.5 lbm/s-in^2 where the specific impulse tends to asymptote at around 200 seconds. This excludes the test conditions for the JAXA RDE hot fires where the data begins to asymptote around 300 seconds at a mass flux value of 0.3 lbm/s-in^2 with outliers at very low flow rates.
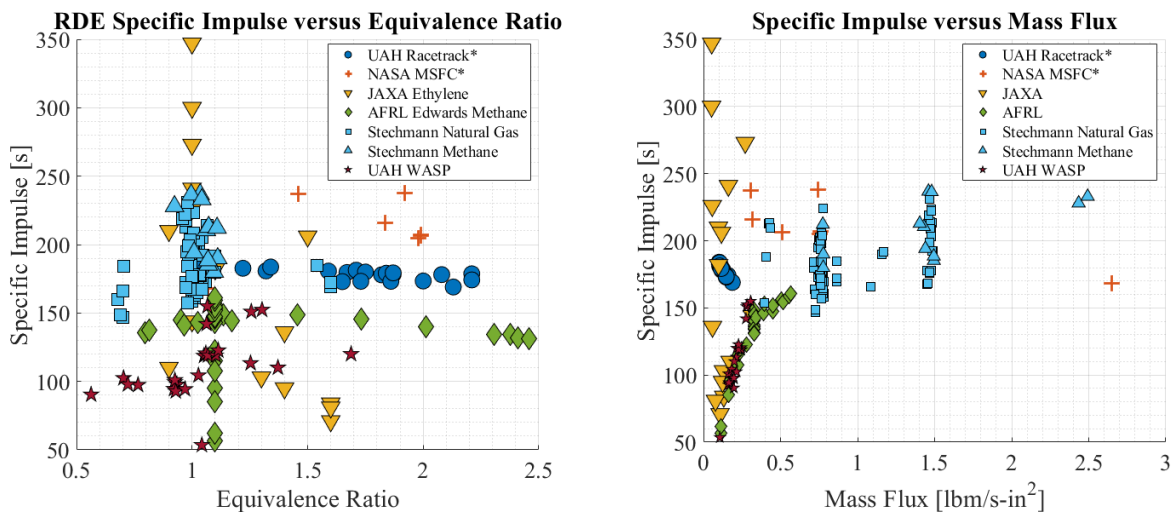
Fig. 3   Left: RDE Thrust vs. Equivalence Ratio for Hydrocarbon Fuel Tests | Right: RDRE Specific Impulse vs Mass Flux for Hydrocarbon Fuel Tests

The next set of comparisons in Figures 4 and 5 are on the detonation wave speed ratio to theoretical wave speed and wave mode of the RDEs at different total mass flow rates and equivalence ratios. This comparison was made to visualize a community rule of thumb that an increase in total mass flow rate increases the wave speed and decreases the number of waves. It can also be seen that the wave "efficiency" or the ratio of actual to theoretical wave speed appears to be at it maximum around stoichiometric conditions. Meaning there is more complete combustion. For the wave mode plot versus equivalence ratio, it can be see that the wave mode of 6 waves is the most common and that wave modes that

6

are an even number are also more common. It was also noted in the analysis that, unsurprisingly, the wave speed and ratio of actual to ideal detonation wave speeds increases with a decreasing number of detonation waves present in the combustor. To attempt to isolate the impact of total mass flow rate and equivalence ratio on detonation wave behavior, only the tests that used methane and oxygen propellants were considered.
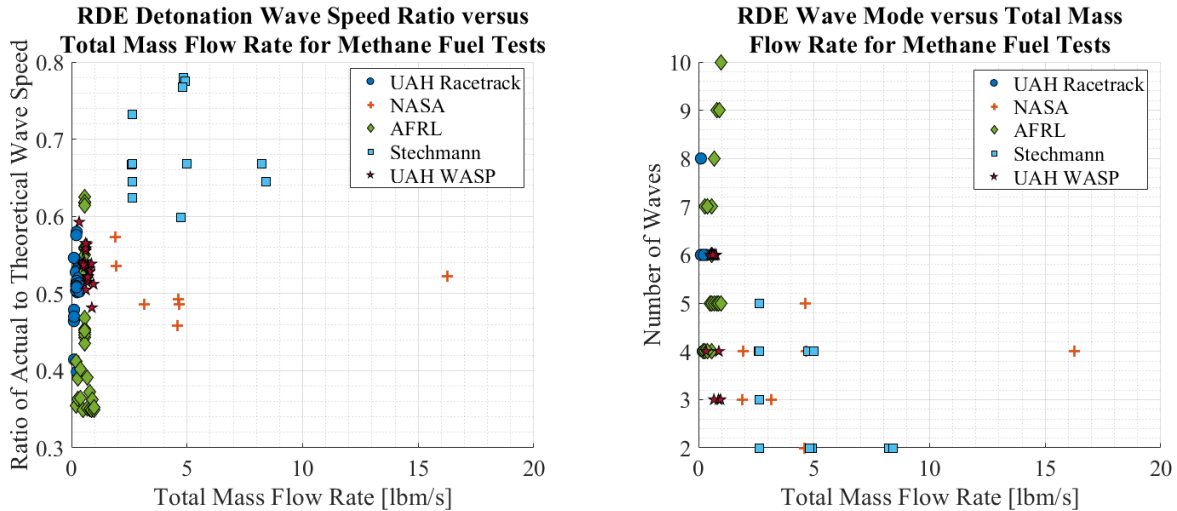

Fig. 4   Left: Wave Speed Ratio vs. Total Mass Flow Rate | Right: Wave Mode vs. Total Mass Flow Rate
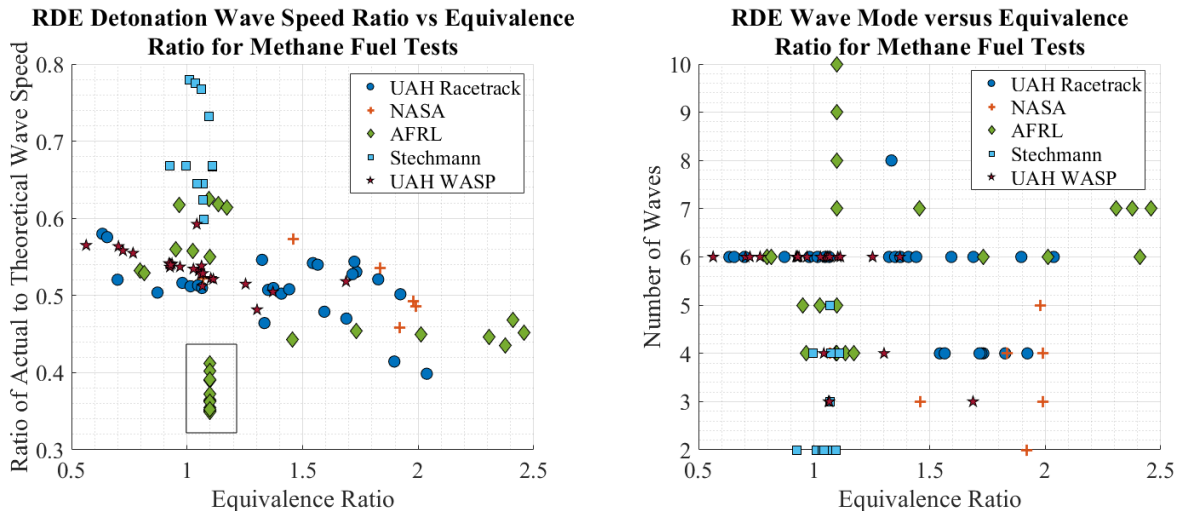
Fig. 5   Left: Wave Speed Ratio vs. Equivalence Ratio | Right: Wave Mode vs. Equivalence Ratio

1. Data Survey of Combustion Efficiency Dependence on Chamber Length

The next set of plots, Figure 6 and Figure 7, look specifically on the impact that chamber length has on the completeness of combustion in an RDE. These plots are divided into tests that reached relatively high chamber pressures and relatively low chamber pressures. A normalized consideration of the gap width and combustor length is compared to what could be considered detonation wave efficiency, or the ratio of actual to theoretical wave speed, and combustion/engine efficiency via the characteristic velocity. For the gap-to-length ratio η to decrease, either the chamber length is longer for the same gap width, or the gap width decreases for the same chamber length. A large value of η could mean either the RDE has a relatively short chamber length or it could have a relatively larger gap width.

7

Conversely, a smaller value of η means a relatively longer chamber length or a relatively smaller gap width. This raises the question of whether or not there is an ideal ratio for proper combustion. It can be hypothesized that the longer the combustion chamber, the reactants have more space and time to complete combustion and will have higher performances than shorter combustion chambers. Chamber pressure would have a large impact on the recovered performance. In the same respect, at a certain point, increasing the combustor length will have little to no more effect on the performance. We know that there is a minimum gap width needed to sustain a detonation depending on the detonation cell size via the propellant type, and many RDEs are designed with this value in mind. A study by Wang et al. found that when investigating the combustor width effect on wave propagation in RDEs that more stable detonations are easier to obtain with larger gap sizes and that the average propagation velocity will decrease as the combustor width is reduced [18]. Finding an ideal gap-to-length ratio would help determine the ideal chamber length. For tests in which the characteristic velocity was not provided, it was calculated using ideal rocket relationships using the following equation:

$$C^* = \frac{P_c A_t}{\dot{m}} \tag{6}$$

Tests that were considered relatively low chamber pressure tests were those that had pressures lower than 75 psig. A couple of tests had very high chamber pressures and could be considered outliers, so to limit the "high" pressure cases, the range observed were tests between 75 psig and 150 psig.
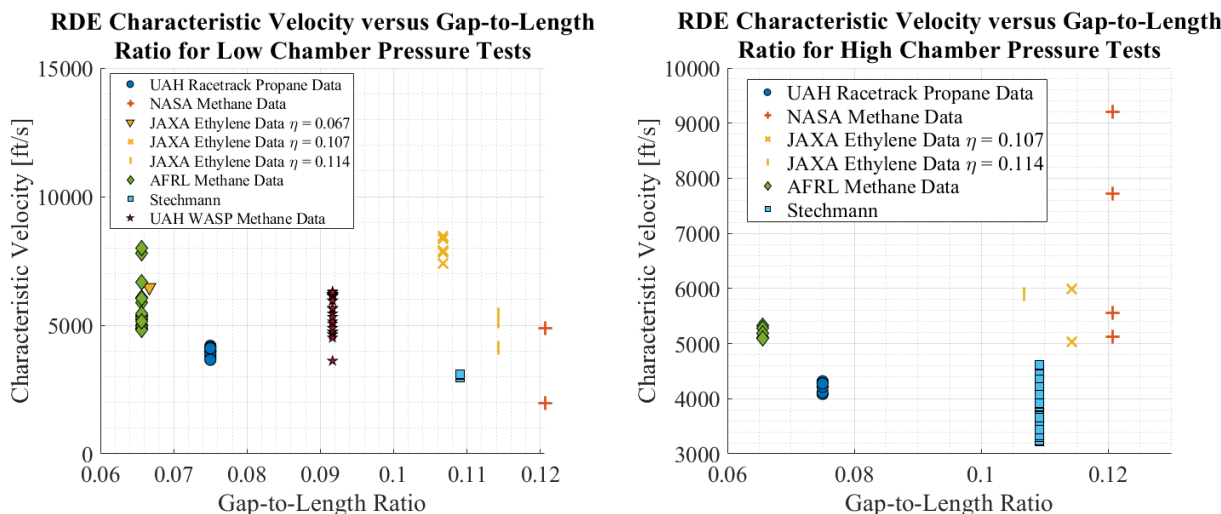
Fig. 6   Left: Characteristic Velocity for Various Gap-to-Length Ratios for Low Chamber Pressure Tests | Right: Characteristic Velocity for Various Gap-to-Length Ratios for High Chamber Pressure Tests

B. Prediction Model

Each prediction model considered three input variables: equivalence ratio, mass flux, and gap-to-length ratios. The trained models were then used to predict chamber pressure, thrust, characteristic velocity, wave speed, and wave mode. With each prediction, a 2D map of two varied inputs and one input held constant was plotted. A table summarizing the variable ranges and constant values of equivalence ratio, total mass flow rate, and gap-to-length ratio are shown in Table 2. The best predictions, meaning the ones with the lowest standard deviations, were the thrust and chamber pressures shown in Figure 9 and Figure 8. The worst predictions, with very high standard deviations, were the wave mode and the wave speed. With three input variables and five prediction variables, 15 2D maps were constructed to visualize the impact of variables on performances. The remainder of the prediction maps are shown in the appendix.

Figure 10 shows the training model results for characteristic velocity for variable gap-to-length ratio and mass flux to compare to the batch plotting analysis in Figure 6. The standard deviations of these results are very high, so it's not a good representation of the prediction of characteristic velocity, but we do see focused areas around gap-to-length ratios of 0.14, 0.11 and 0.06.

The following figures use the prediction model that was built to predict the performance of the UAH WASP engine. The chamber pressure, thrust, characteristic velocity, and wave speed are predicted. The plots of prediction versus truth

8
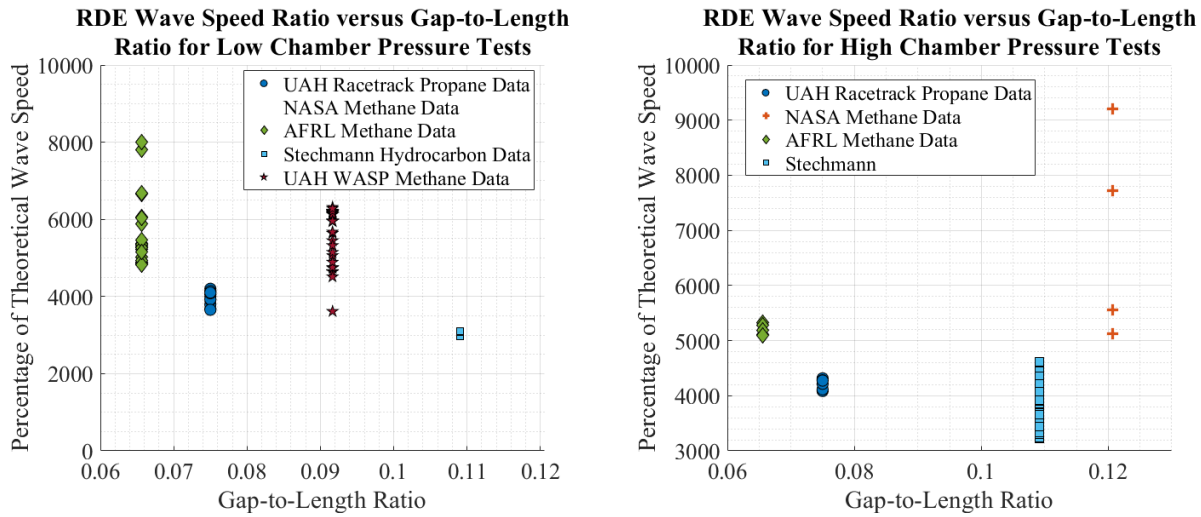
Fig. 7   Left: CJ Velocity Ratio for Various Gap-to-Length Ratios for Low Chamber Pressure Tests | Right: CJ Velocity Ratio for Various Gap-to-Length Ratios for High Chamber Pressure Tests

	Constant ϕ	**Constant $\dot{m}'$ $\frac{lbm}{s-in^2}$**	**Constant η**
Constant Value	1.1	1.5	0.12
	Variable ϕ	**Variable $\dot{m}'$ $\frac{lbm}{s-in^2}$**	**Variable η**
Variable Range	0.5 - 2.0	0.0 - 3.0	0.06 - 0.15

Table 2   Summary of Constant and Variable Input Conditions for Prediction Model

data are shown below. If the model perfectly predicts the test data, all of the points should fall on the dotted line. The predictions of thrust and chamber pressure are adequate, but for wave speed and characteristic velocity the values are highly under-predicting.
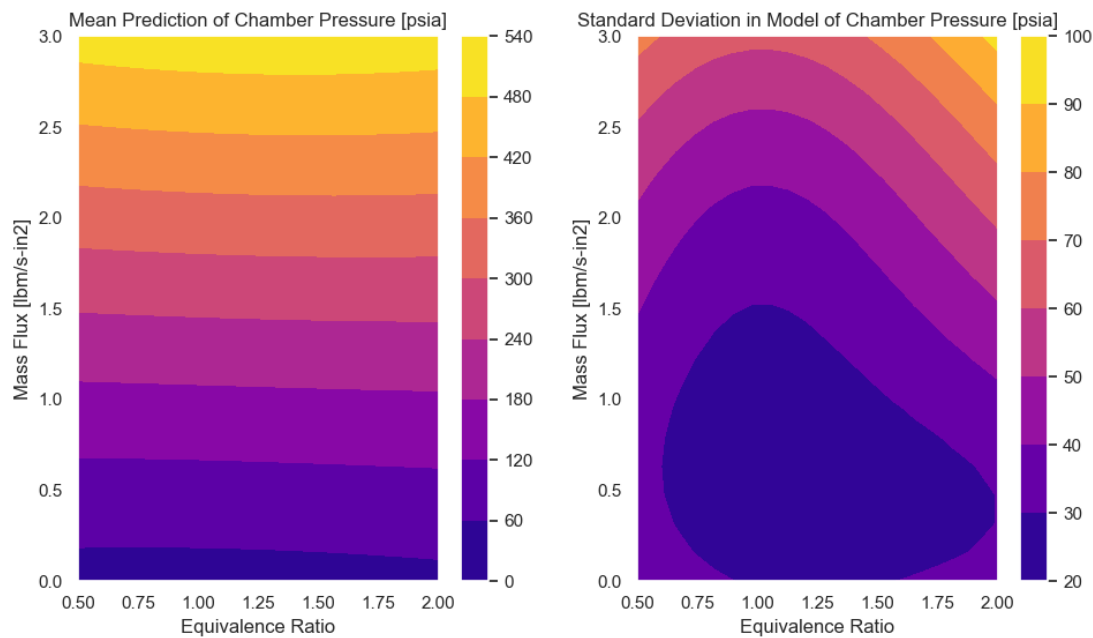
Fig. 8   Left: Prediction of the Chamber Pressure for Variable Total Mass Flow Rate and Equivalence Ratio, Gap-to-Length Ratio = 0.12 | Right: Standard Deviation of the Chamber Pressure Prediction
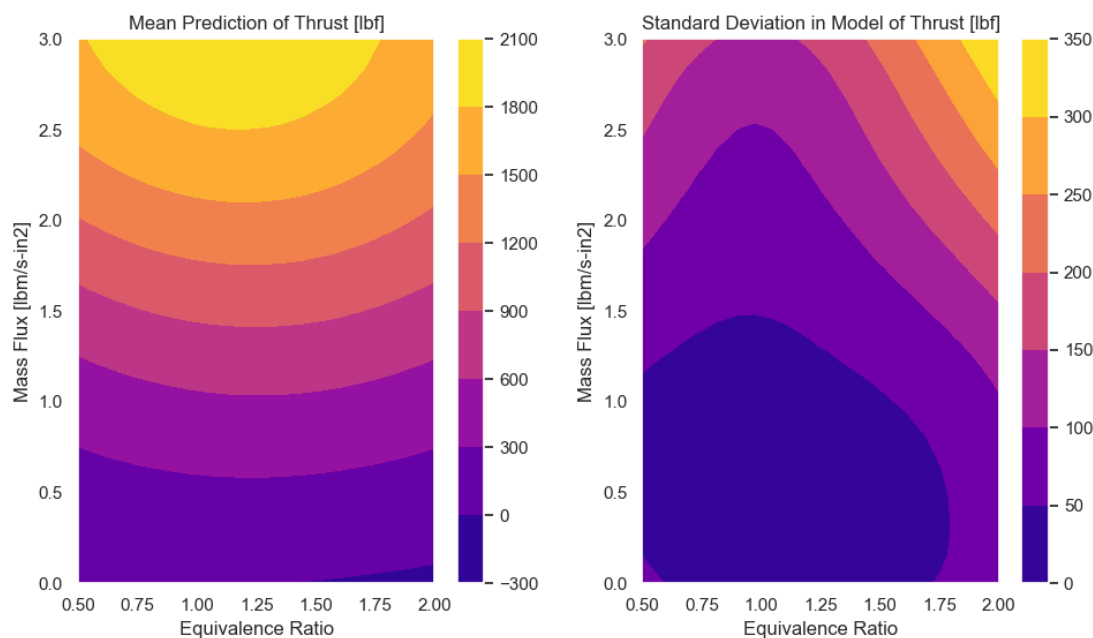
Fig. 9   Left: Prediction of the Thrust for Variable Total Mass Flow Rate and Equivalence Ratio, Gap-to-Length Ratio = 0.12 | Right: Standard Deviation of the Thrust Prediction

10
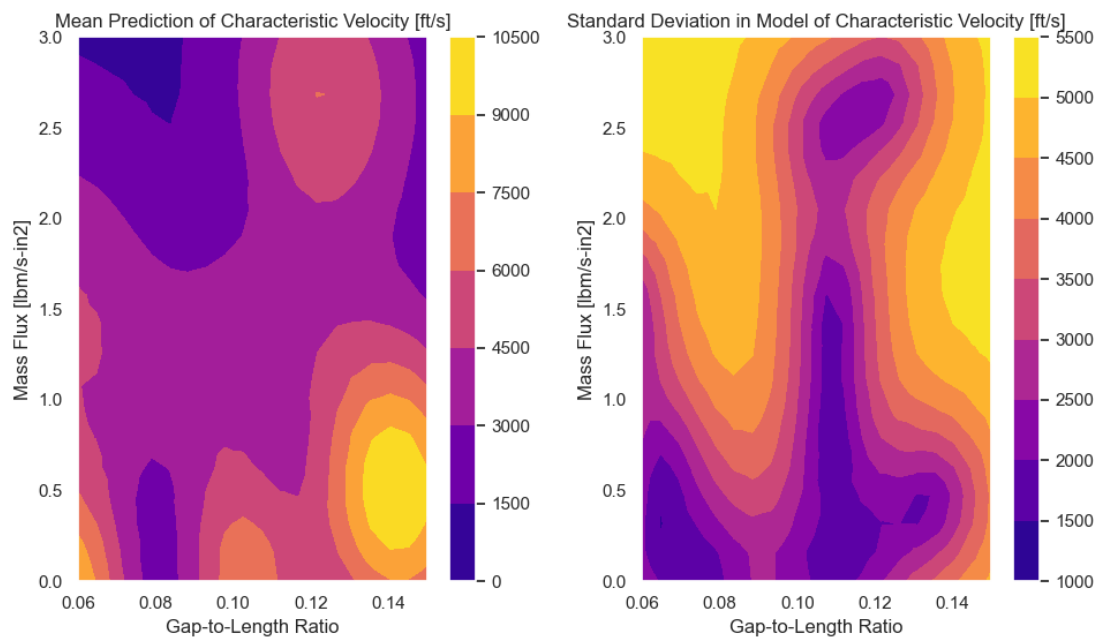
Fig. 10   Left: Prediction of the Characteristic Velocity for Variable Total Mass Flow Rate and Gap-to-Length Ratio, η, at an Equivalence Ratio of 1.1 | Right: Standard Deviation of the Characteristic Velocity Prediction
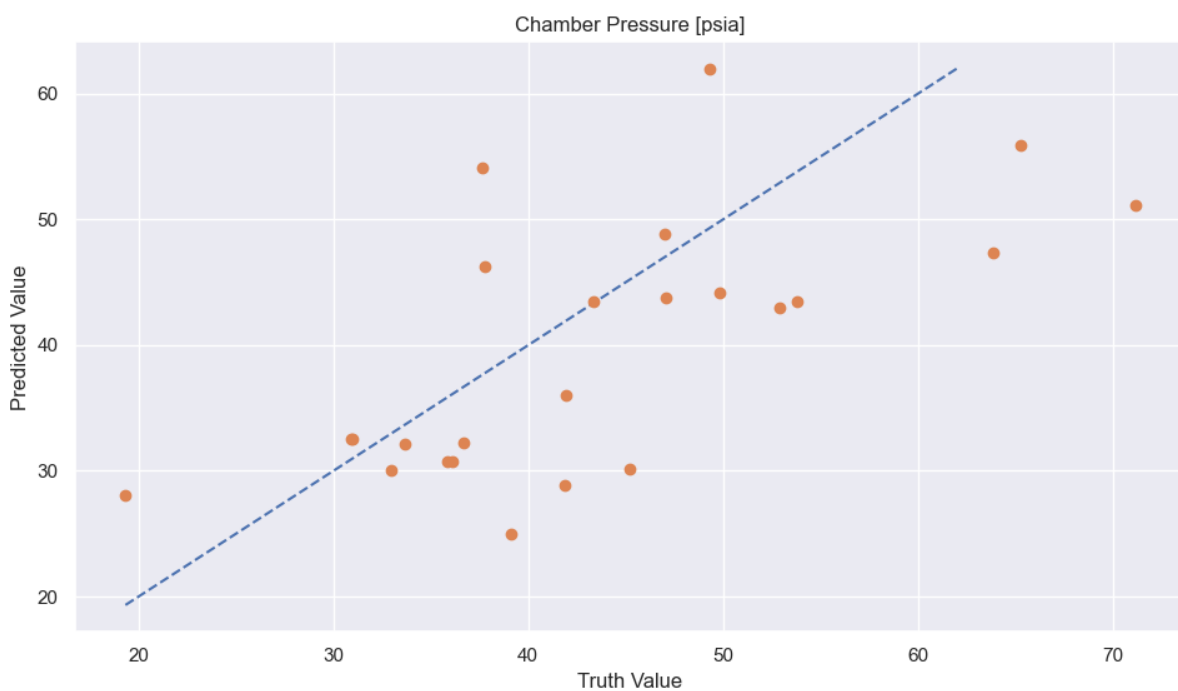
Fig. 11   Prediction Model Results of Chamber Pressure

11
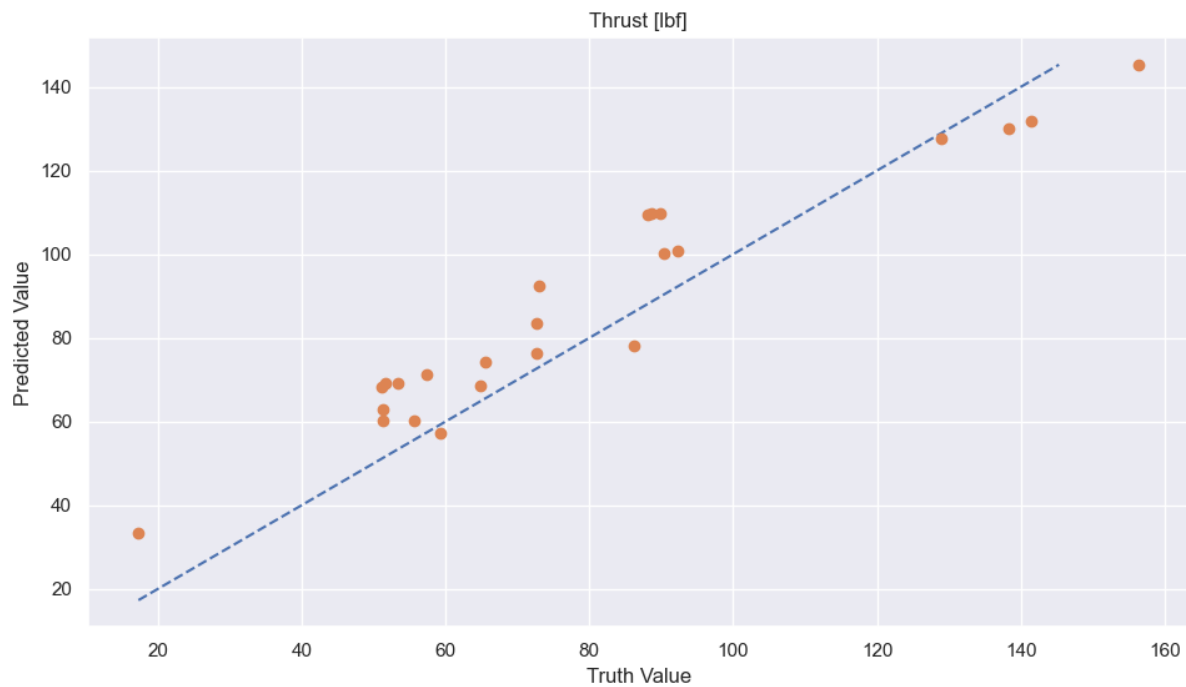
Fig. 12   Prediction Model Results of Thrust
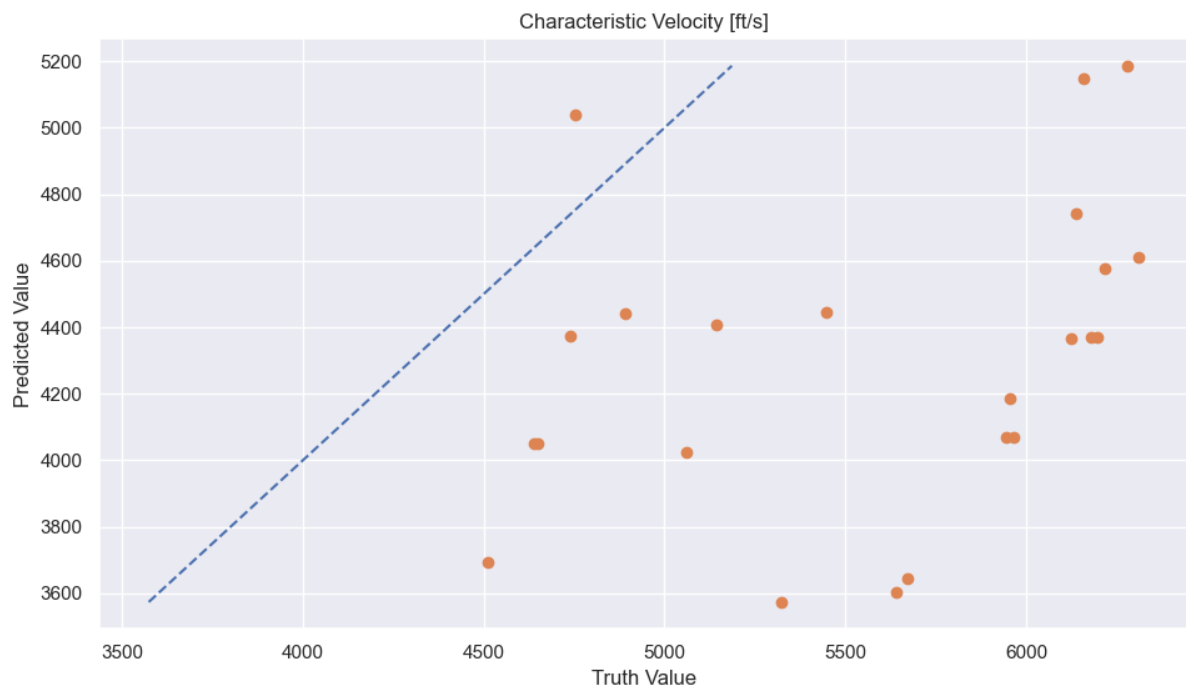
Fig. 13   Prediction Model Results of Characteristic Velocity

12
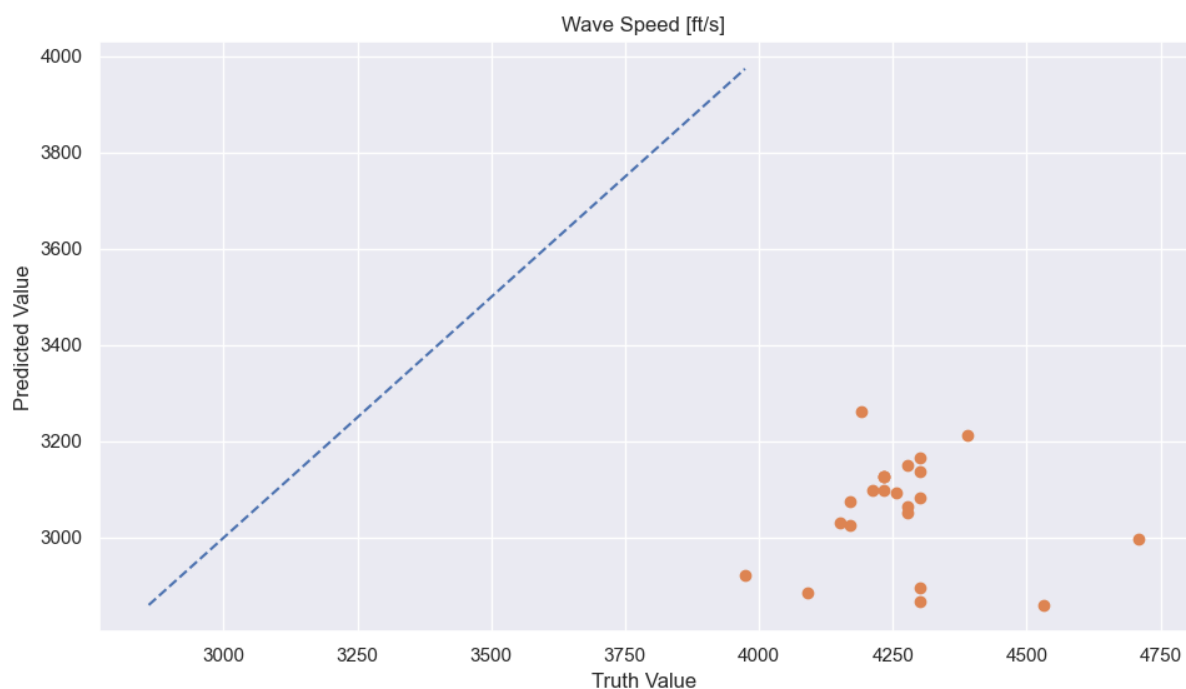
Fig. 14   Prediction Model Results of Wave Speed

V. Discussion

A. Literature Survey

In general, the literature survey and comparison analysis of the data found some interesting relationships, some expected. Based on what we know about hot fire tests of RDEs, we can observe the relationship of engine performance such as chamber pressure, thrust, and specific impulse. This gives confidence in predicting the engine performance. However, based on experience, the wave mode and wave speed are much more difficult to predict. There is a loose relationship of fewer waves with increasing mass flow rate. It can be seen with fewer waves that the wave speed is closer to the theoretical, CJ wave speed. Some of the results showed that if a test resulted in a 1-wave mode, the wave speed was 90% to just over 100% of the CJ speed. A detailed discussion of each figure will be discussed here.

Looking at the test matrix mapping of each hot fire campaign we can see that low total mass flow rates have been prioritized for open source literature. That's not to say that higher total mass flow rates haven't been tested. Those test conditions lead to higher chamber pressures and thrust output, so it's likely that that work has been published in closed forums. Not surprisingly, most of the tests have been centered around stoichiometric mixes of propellant given that it means complete combustion. There is a slight shift towards more rich conditions because it has been noted by some research efforts show that the highest performance for methane and oxygen propellants actually comes from an equivalence ratio of around 1.1 or slightly greater [13] [19]. Most test campaigns target richer propellant conditions compared to lean conditions. The group out of AFRL Edwards claims in their publications that for the most lean conditions, performance drops off by 34% while at the most rich conditions, performance drops off by 8% [13]. This could explain why most research efforts avoid lean conditions in hot fire tests.

As expected, there is a linear increase in thrust with total mass flow rate. When the effect of chamber cross-sectional area is included, there is a noticeable deviation resulting in what appears to be two linear relationships with different slopes. For the upper linear trend, for a 0.7 lbm/s-in^2 increase in mass flux, it's expected that there will be an increase of 500 lbf of thrust. Meanwhile, for the lower slope a 0.7 lbm/s-in^2 increase in mass flux leads to an expected thrust increase of 125 lbf. Upon a closer look at the thrust and mass flux plots in Figure 2, the data points that appear to be on the "lower" linear relationship are from the tests conducted at ARFL and some of the tests of Stechmann's dissertation. The geometry of those tests are shown Table 3. At a first look, the trend appears to be due to the similar gap-to-length ratios. This would lead one to conclude that the larger ratios lead to less thrust for a given mass flux. However, that conclusion fails when looking at the hydrocarbon tests performed by Stechmann where the ratio is much less. The next conclusion that may be tempting to make is that it involves smaller gap widths, but the group by AFRL has a much larger gap width. Lastly, the AFRL group and the hydrocarbon tests by Stechmann have similar combustor cross sectional areas, but the hydrogen test area is smaller. This behavior of thrust and mass flux could be because the gap widths are considered somewhat "off-nominal." A gap width of 0.1 or 0.15 inches is relatively small, and the gap width of nearly 0.4 inches is fairly large. However, this could be a balance of the gap width and the gap-to-length ratios that could also be causing this behavior where these deviate from the original linear trend as seen with the total mass flow rate plot.

Test Identifier/Group	Gap-to-Length Ratio	Gap Width [in]	Cross Sectional Area [in^2]
AFRL	0.131	0.394	1.73
Stechmann Hydrogen	0.133	0.100	1.19
Stechmann Hydrocarbon	0.055	0.150	1.76

Table 3   Geometry of Tests that Resulted in "Lower" Linear Trend of Thrust vs. Mass Flux

The relationship of engine specific impulse for changing equivalence ratio shows that the highest specific impulse output from an engine occurs near stoichiometric mixture conditions. There's not enough here to substantiate the claim that highest performance, in fact, comes from an equivalence ratio of 1.1. Knowing that there's a more substantial drop in performance at lean conditions than rich conditions, there does appear to be a more drastic drop-off in specific impulse on the lean side of the plot versus the rich. However keeping in mind that the majority of the tests were completed at rich conditions, so there may not be enough data to confirm that behavior across different engine geometries and propellants. The higher magnitude thrust output from Stechmann's work is due to the higher total mass flow rates performed. Specific impulse tends increase with mass flow and mass flux but has an asymptotic behavior at higher flow rates. This is shown in Figure 3 with the exception of some of the JAXA results. The difference in the JAXA performances could be because there were much fewer data points for those tests, but also because that test campaign

had different gap-to-length ratios. The higher values of specific impulse were the ones with the higher flow rates but the shorter chamber length. In general, most tests seem to asymptote to between 175 s and 300 s. This is almost the same specific impulse range for typical solid rocket motors.

Moving away from the traditional rocket engine performance metrics. The next couple of figures, Figure 4 and Figure 5, show the performance of a detonation wave compared to the set test conditions. Specifically on the wave mode versus total mass flow rate plot, at similar total mass flow rates, there is a substantial range of possible wave modes that could occur during testing. It could be at slightly different equivalence ratios, or it is potentially a case where some tests have nozzles and some do not. A future look at nozzle configurations could help determine that impact on wave mode. Depending on how the group goes about determining wave mode and wave speed, there is a lot of room for error. If these values are determined only by high-speed imaging, there is a level of subjectivity there that could cause a difference in results. Comparing high-speed imaging results with dynamic pressure measurements can reduce this effect. A group out of AFRL Wright Patterson investigated RDE operation using hydrogen and air to determine propagation velocity and found that for a given total mass flow rate, propagation velocity decreases with decreasing equivalence ratio [20]. Although the set conditions chosen for Figure 5 are not at a constant total mass flow rate, this behavior that the wave speed with respect to it's theoretical speed is decreasing can be observed. An exception to this behavior is marked where some of the tests performed by AFRL at an equivalence ratio of 1.1 had significantly lower wave speeds. These tests were ran at a mix of high and low total mass flow rates, but they all resulted in higher wave numbers which would decrease wave speed. It is unclear why this is happening other than that the engine possibly is being tested at off-nominal flow rate conditions. Propellant mixing has been shown to affect the wave formation in an RDE according to work published through Xiamen University. Quality mixing leads to a decrease of fuel accumulation and avoids localized hot spots. Hot spots have been shown to lead to the formation of multiple detonation waves. So, when there is quality mixing and complete combustion, there should be fewer waves near stoichiometric conditions. Although off-nominal equivalence ratios can lead to multiple detonation waves, multiple waves can be used to stabilize the thrust [21]. This work also claims that as the equivalence ratio increases, the number of detonation wave also gradually increases. The data comparisons in this paper aren't enough to substantiate that claim, but what can be seen is that the most common detonation wave number is 6. Wave modes tend to show up in even numbers with some exceptions. Most of the instances of 6 wave modes come from the UAH WASP testing. Without those set points, the 4 wave mode is the next most common. A potential difference between them are slightly elevated total mass flow rates, but there doesn't appear to be a clear reason why some have 6 modes and some have 4. The other engines are slightly larger in chamber cross-sectional area. A plot that was not included, but was observed when performing the analysis was that as the number of waves increases, the speed of the waves decrease compared to theoretical wave speeds. A group at the University of Cincinnati found that at higher numbers of waves, the head of the waves behave more like acoustic waves rather than detonation waves [22] and could explain the slower wave speeds. This work provided a summary of properties that affect wave performance and cited that co-rotating waves are theorized at higher flow rates. That data that we have shows an even distribution of co-rotating and counter-propagating waves although most test cases were performed at low flow rates.

A consideration of chamber length and the engine channel gap to chamber length ratios and how that affects the efficiency of the combustion in an RDE is being considered. Therefore, this work takes a look at how the gap-to-length ratio impacts efficiency for both engine and detonation by looking at the engine chamber pressure and characteristic velocity for engine performance, and wave speed ratio for detonation wave performance. It is expected that a longer chamber length is necessary to allow for complete combustion. There is more volume for the reactants to combust before it exits the engine chamber. To normalize the behavior when considering chamber geometry, the gap-to-length ratio was chosen over the chamber length alone. The percentage of recovered performance when considering characteristic velocity is heavily dependent on the chamber pressure of the engine. For high pressures and higher gap-to-length ratios, it has been shown that the percentage of recovered performance increases a small amount, while for the same higher chamber pressures and a decrease in the gap-to-length ratio, the percentage of recovered ideal performance increases greatly. The figures show for similar chamber pressures, a comparison of "high" and "low" relative chamber pressure, when comparing performance for geometry ratios to see if the literature supports this claim. A comparison of the actual characteristic velocity compared to ideal, so the percentage of performance recovered would be a better comparison, but some of these values for characteristic velocity are already estimated based on the information that was provided. In some plots there does appear to be a loose correlation between larger gap-to-length ratios and better engine and wave performance. When looking at characteristic velocity, the gap-to-length ratios of around 0.11 and 0.13 tend to peak at low pressure tests and 0.12 at high pressure cases. The wave speed ratio shows a peak greater than 0.13 for low pressure and 0.12 again for high pressure. Future experimental tests will be looking at this behavior.

15

B. Prediction Model

At this time, the best predictions are of the chamber pressure and thrust performance of an RDE followed by characteristic velocity. What is surprising about how good the predictions are for thrust and chamber pressure is that it appears to be independent of the injector type, nozzle configuration, and propellant. Therefore, the thrust appears to be insensitive to engine design. The predictions of wave mode and wave speed have extremely large standard deviations and therefore cannot be considered accurate predictions of the wave activity in an RDE. Figure 9 does show us that slightly less mass flux is necessary to reach a thrust output at an equivalence ratio of around 1.25. Some previously cited work did discuss that hydrocarbons tend to reach max performance at slightly richer propellant mixtures. This modeling effort, however, also looks at fuels such as hydrogen. Also the standard deviation around equivalence ratio equal to one is low. This is good and is expected as most of the data is clustered here driving the confidence of the model upwards.

The prediction of characteristic velocity with variable mass flow rates and gap-to-length ratios is highlighted in the results and discussion to compare to the survey results. While the prediction itself is not as good as the thrust and chamber pressure, it does highlight that a gap-to-length ratio of around 0.14 would yield the best results followed by a ratio of about 0.1 to 0.11 and then 0.06. A ratio of 0.14 could mean that either an RDE with a shorter chamber length or a larger gap width would yield better results.

In the prediction of the UAH WASP RDE hot fire results, the predictions of chamber pressure and thrust are okay while the characteristic velocity and wave speed are not good predictions. A summary of the MAE of each prediction is shown in Table 4. The prediction accuracy could be due to assumptions of standard deviation, lack of diverse data points, or, for especially for wave activity, the natural chaotic nature of detonation waves.

	Chamber Pressure	Thrust	Characteristic Velocity	Wave Speed
MAE	8.11 psi	11.35 lbf	1281 ft/s	1207 ft/s
Percent Error of Average	19%	14%	23%	28%
Percent Error of Maximum	11%	7%	20%	26%

Table 4   Mean Absolute Error and Percent Error of Average and Maximum Performance of the UAH WASP RDE Predictions

During model creation the errors for some of the better performing models is less than 6% of the range of predictions (see MAE in figure 18. The 95% confidence interval is also about ± 4% for those models. Both of these meet the rule of thumb of less than 10% error meaning the models capture first order effects and trends. Because of these measurements, the authors see the better performing models as acceptable with room for improvement.

The high variance of the model in some of the predictions may be due to any of the following issues: more data spanning the design space, better uncertainty estimates, reducing uncertainty in data collection and system testing, improved measurements, different independent variables, or further optimization of the Kriging model. If one is looking to improve the quality of the model one may target one or more of the areas of improvement.

Kriging models can include uncertainty priors when training the model. Ideally, each point would have an associated uncertainty, but the cost to generate those distributions is too great. However, measured uncertainty at one point can be used to approximate the uncertainty of an experiment set. This uncertainty can then be applied to each data point gathered from the same testing apparatus. This is of paramount importance to measuring the quality of the measurement and building a higher performing model. The authors request that the community take multiple non-consecutive samples (7-9) at one set point throughout the testing campaign to capture the uncertainty of the testing system and report that with all future findings. This version of a repeatability study is a good balance between experimental cost and producing usable and high quality data.

VI. Conclusion

This work aimed to take a look at existing RDE hot fire data from around the world and use it for two things: a literature survey data comparison of performances to isolate behaviors that are worth a closer experimental work, and to use the data to train a machine learning model to attempt to predict the performance of UAH's recently hot fired RDE. The data comparisons were divided into engine performance, so values such as chamber pressure, thrust, specific impulse, and characteristic velocity, and detonation wave performance like wave speed, wave mode, and percentage of theoretical CJ wave speed. Batch plotting in this way confirmed some of the claims made by other groups, and a

specific look at chamber length or gap-to-length ratio and the influence that has on performance will serve as a basis of comparison for future tests on the UAH WASP engine.

Prediction modeling efforts show that there is evidence, but not proof, of an adequate model for engine performance such as chamber pressure and thrust. However, the predictions for wave mode and wave speed are not good predictions with very large standard deviations. Therefore, when predicting the WASP RDE data, the predictions of chamber pressure and thrust have relatively low MAE, while the MAE for characteristic velocity and wave speed are very high.

Some ways improve this work are to identify a consistent and clear way to report on hot fire performance. Another way to get a more accurate look at wave performance is to find a way to remove the subjectivity of determining wave modes especially when there is a lot of parasitic deflagration present and there is the presence of strong vs. weak detonation waves in high speed imaging. Repeatability tests, while time consuming and expensive, are vital when attempting to construct prediction models. This work was working with over 200 data points, which for most prediction model efforts, is a sufficiently large set, however it's not the number of data points, it's the diversity of where those data points are coming from i.e. different engine sizes and designs.

Future work on this analysis would be to continue to locate data that can be included in the analysis to attempt to improve the predictions of all performance parameters. The authors also wish to explore high flow rate data and further work on chamber length studies. With a larger number of diverse data sets, taking a look at batch plots of injector types and injector performance as well as different nozzle configurations could prove useful. This work excluded the impact of injectors and nozzles which can have large impacts on performance especially wave modes. The prediction model also incorporated all propellant types. In the future, batching the prediction into hydrocarbons compared to hydrogen fuels could yield different results. Future work will also include Principle Component Analysis (PCA) as a way to weigh the importance of each variable on predicting RDE performance. This would determine what variable (geometry or set condition) has the largest impact in performance. The model can be used for an adaptive log-likelihood sampling for model improvement. This can drive sampling areas of the model that provide the most potential to improve engine performance.

Appendix

All of the code to create the models are available on github at `https://github.com/nhemming/RDRE_Injector_Modeling` . It does not require any python experience to run as it is setup to be input file based. The following open source packages were used for creating the models in this paper: matplotlib [23], numpy [24], pandas [25], scikit-learn [26], seaborn [27].

A. Prediction Maps and N-Fold Cross Validation Plots

The 2D maps and 10-fold cross validation plots for chamber pressure, thrust, characteristic velocity, wave speed, and wave number, respectfully, are shown in the figures below.
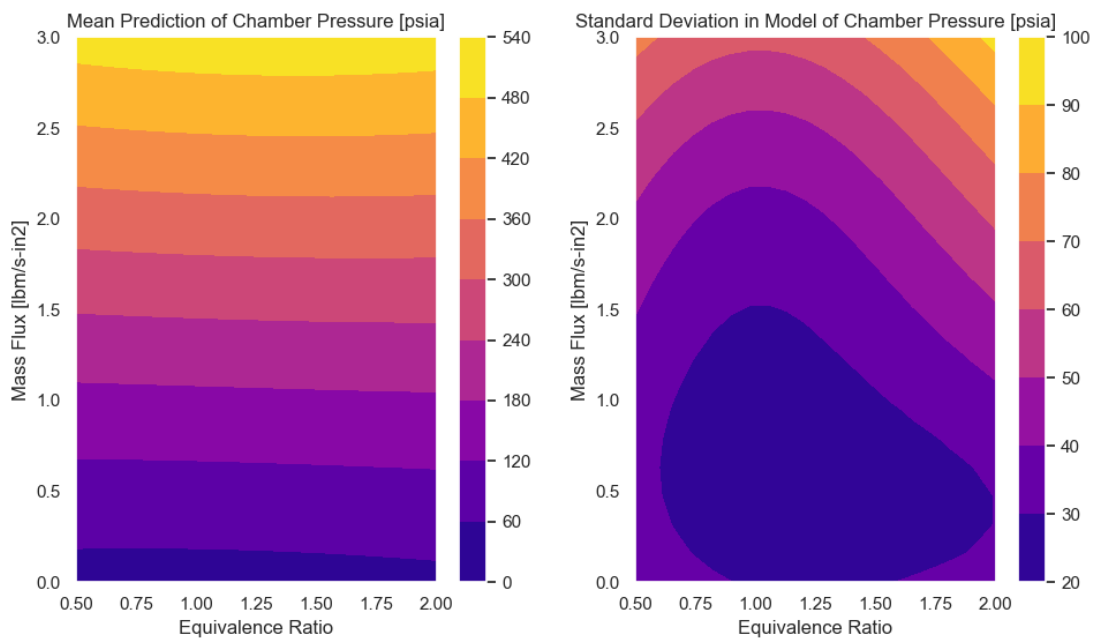
**Fig. 15   Chamber Pressure Prediction for Constant η**
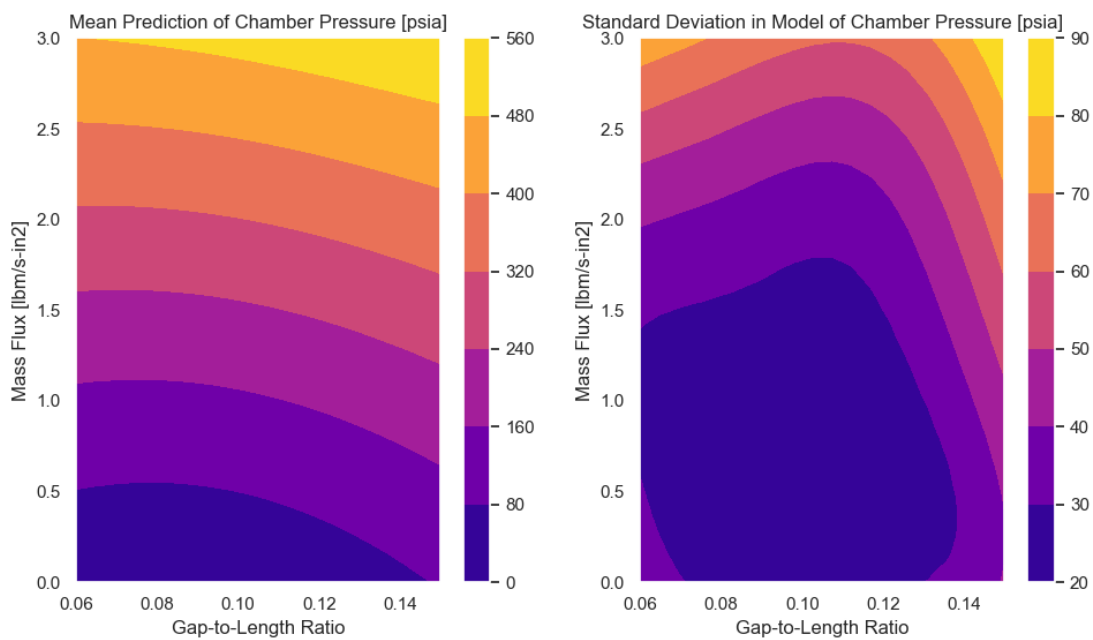

Fig. 16   Chamber Pressure Prediction for Constant ϕ
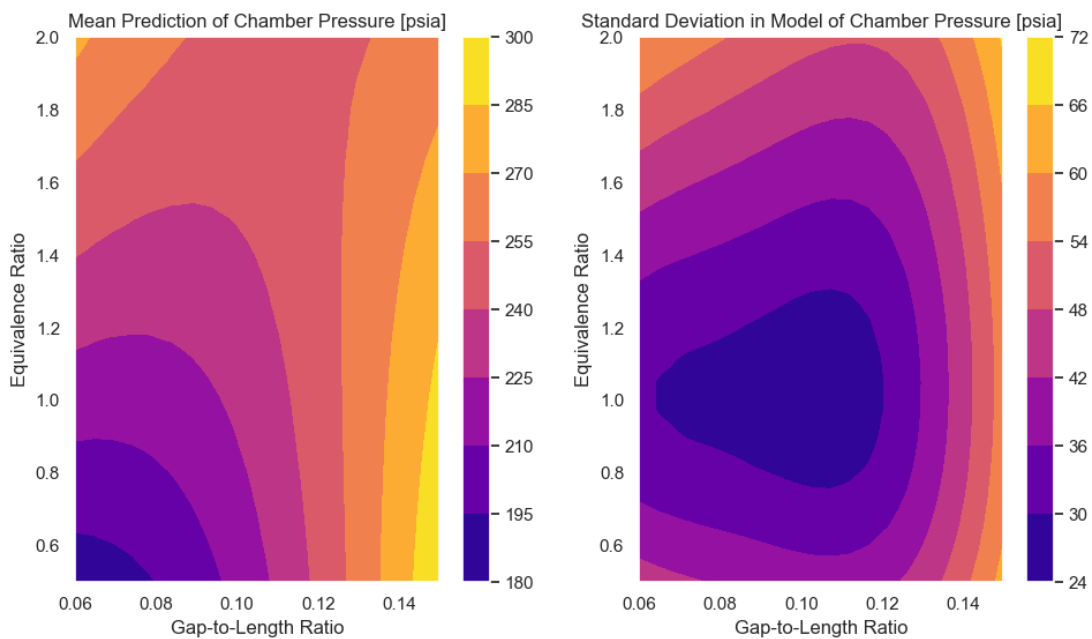
18

Fig. 17   Chamber Pressure Prediction for Constant $\dot{m}_T$
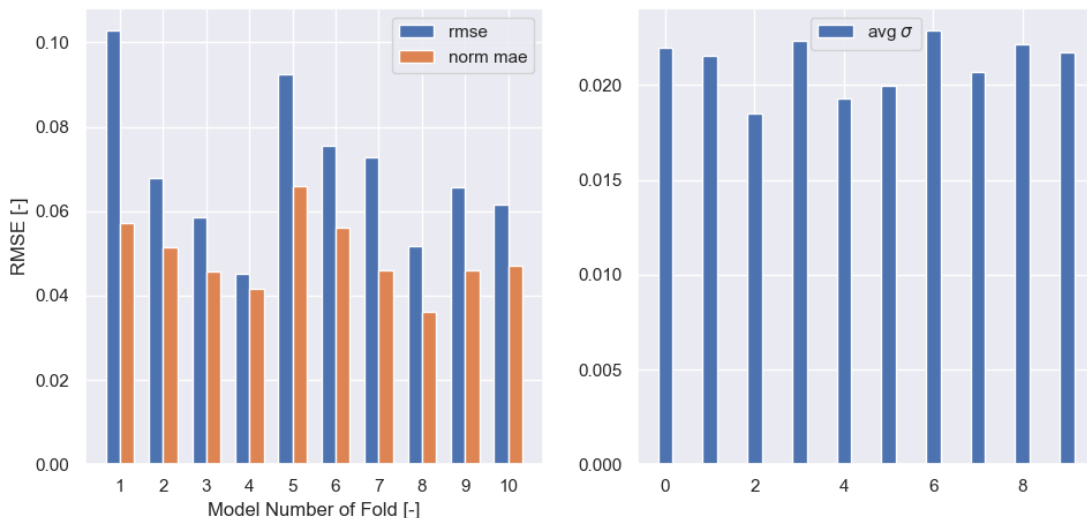

Fig. 18   N-Fold Error Analysis of Chamber Pressure Prediction
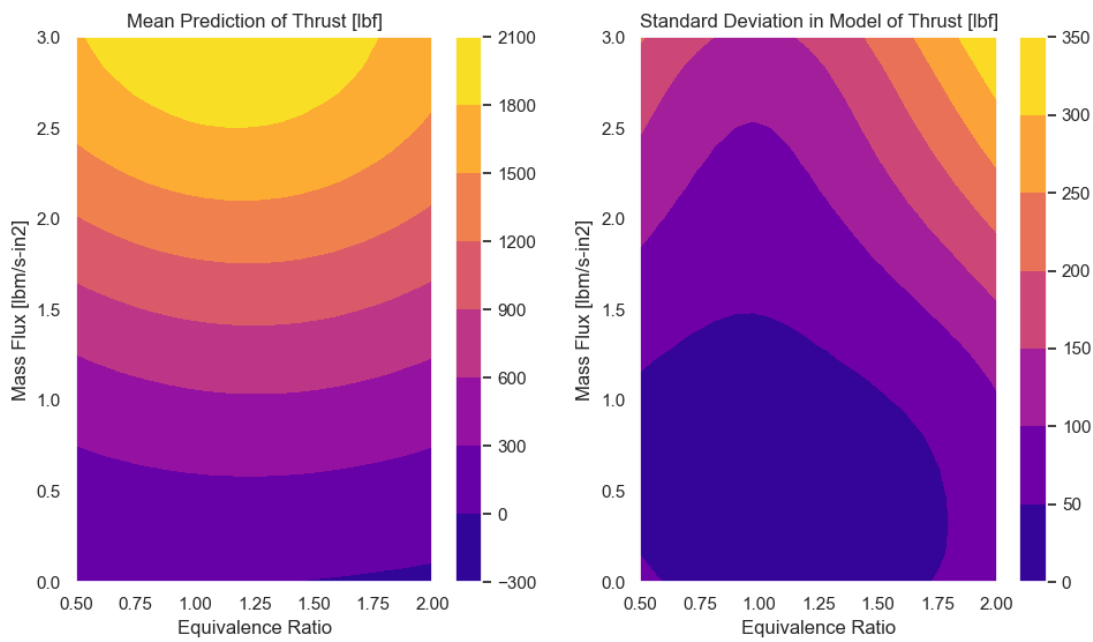
Fig. 19   Thrust Prediction for Constant η
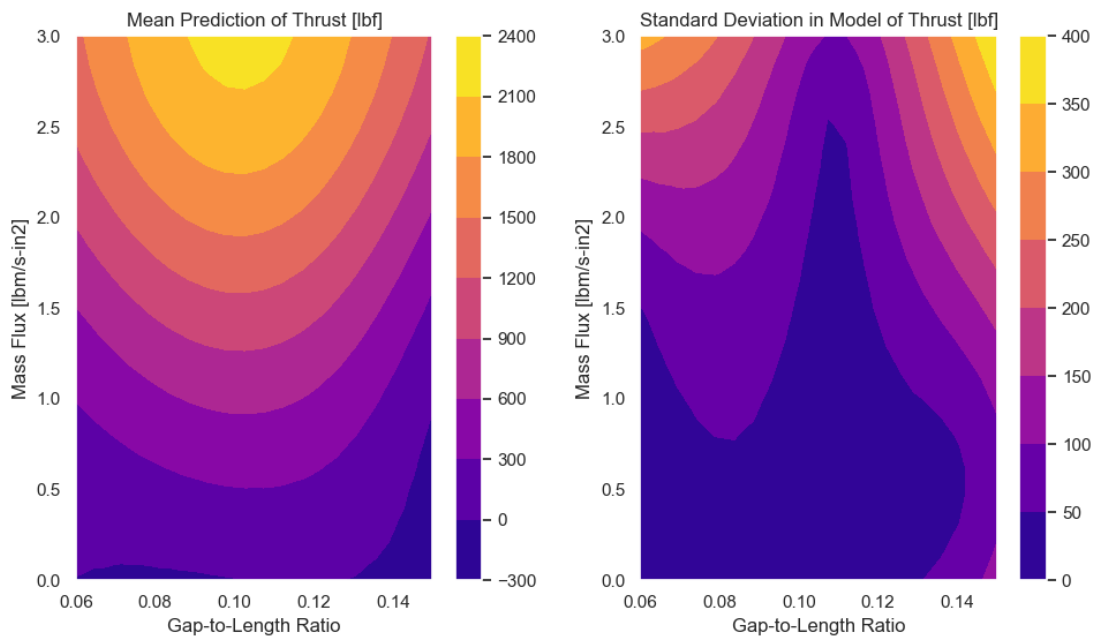
**Fig. 20   Thrust Prediction for Constant** ϕ
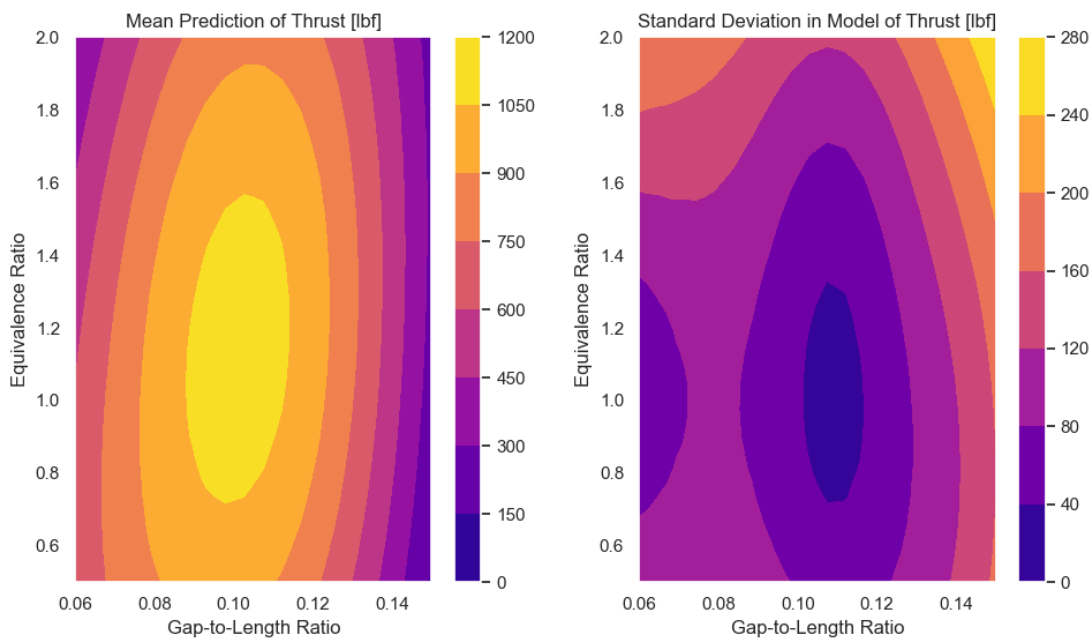
Fig. 21   Thrust Prediction for Constant $\dot{m}_T$
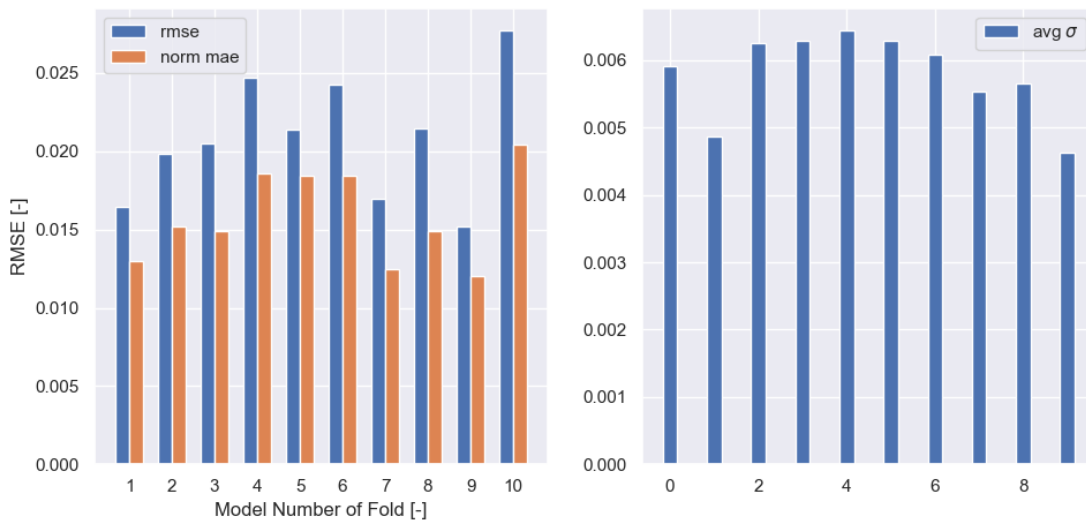
Fig. 22   N-Fold Error Analysis of Thrust Prediction

21
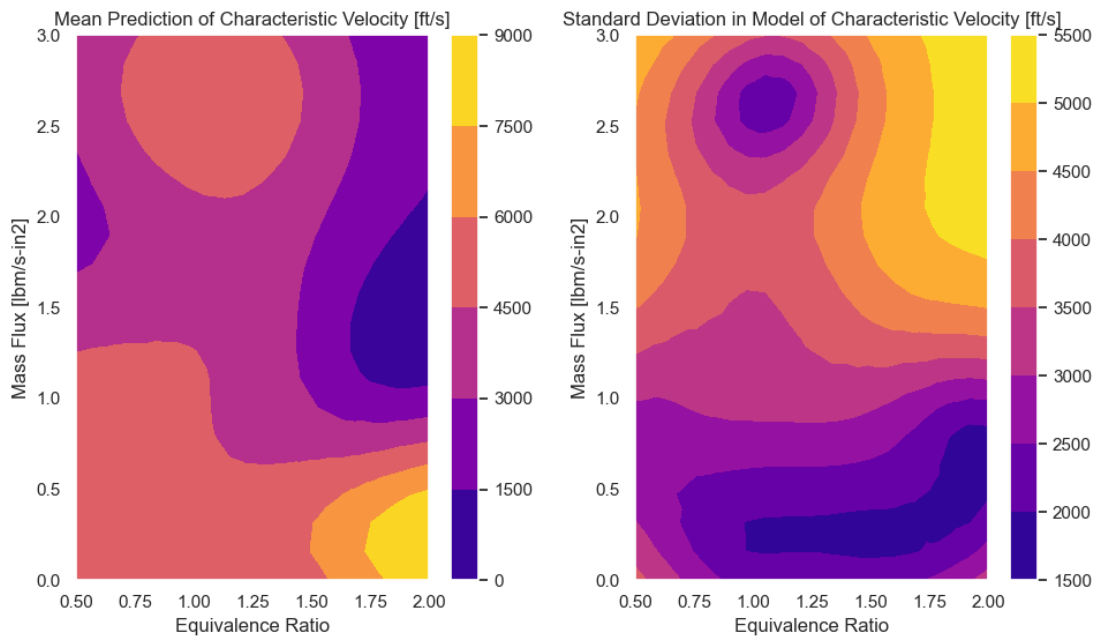
Fig. 23   Characteristic Velocity Prediction for Constant η
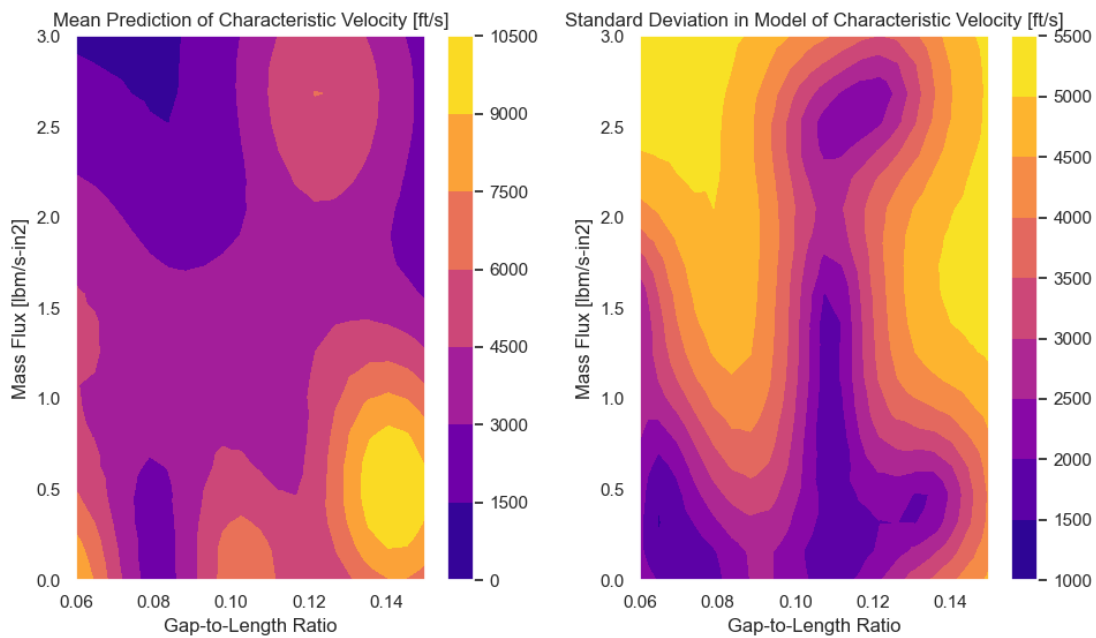
Fig. 24   Characteristic Velocity Prediction for Constant ϕ
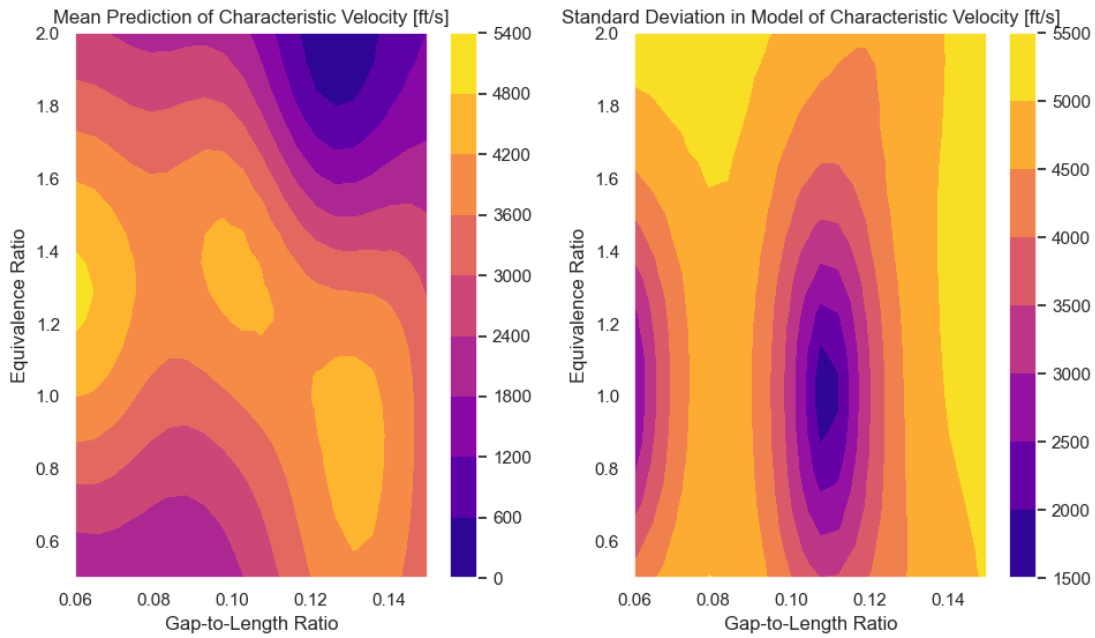
Fig. 25   Characteristic Velocity Prediction for Constant $\dot{m}_T$
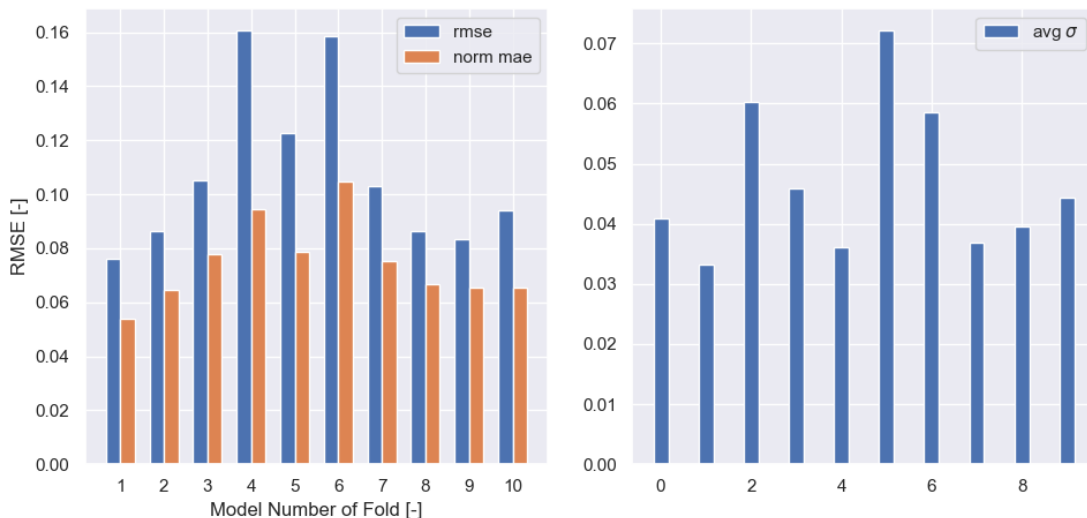
Fig. 26   N-Fold Error Analysis of Characteristic Velocity Prediction
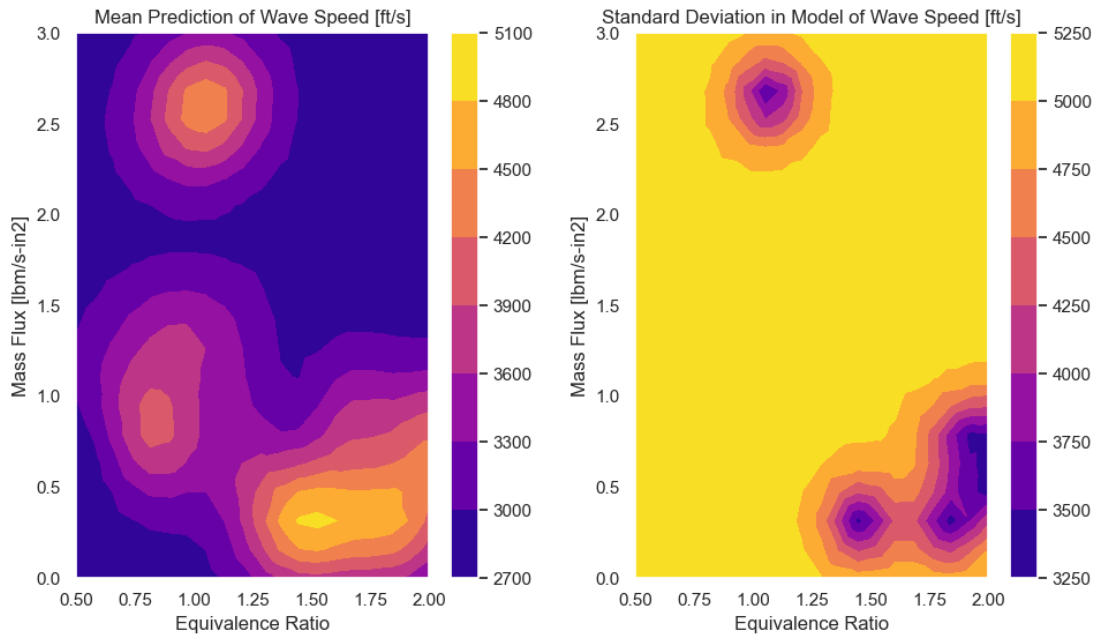
Fig. 27   Wave Speed Prediction for Constant η
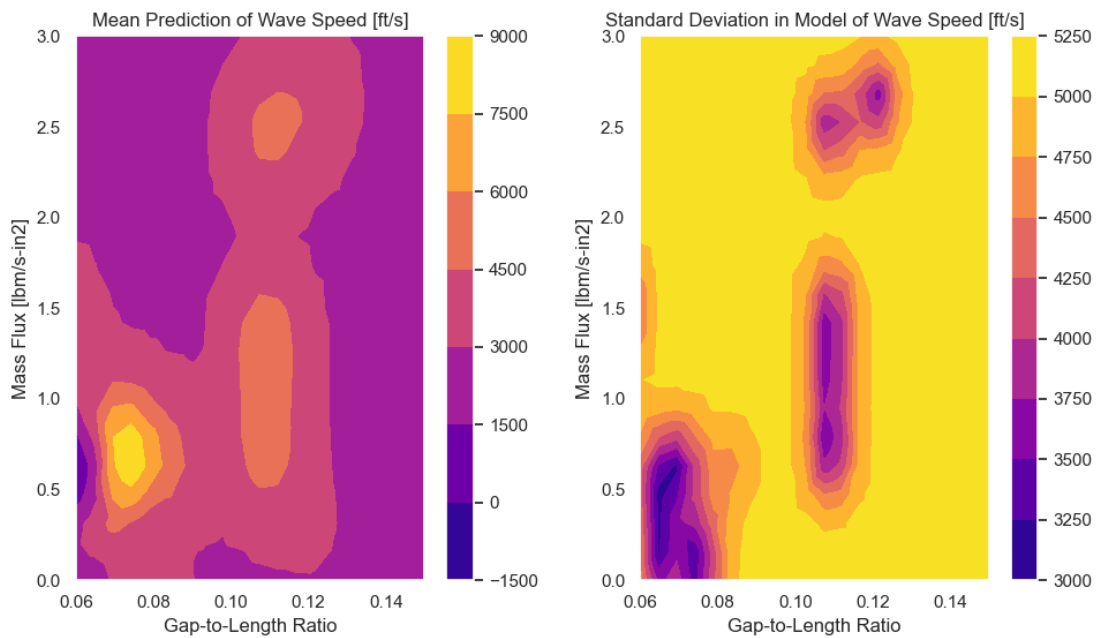
Fig. 28   Wave Speed Prediction for Constant ϕ
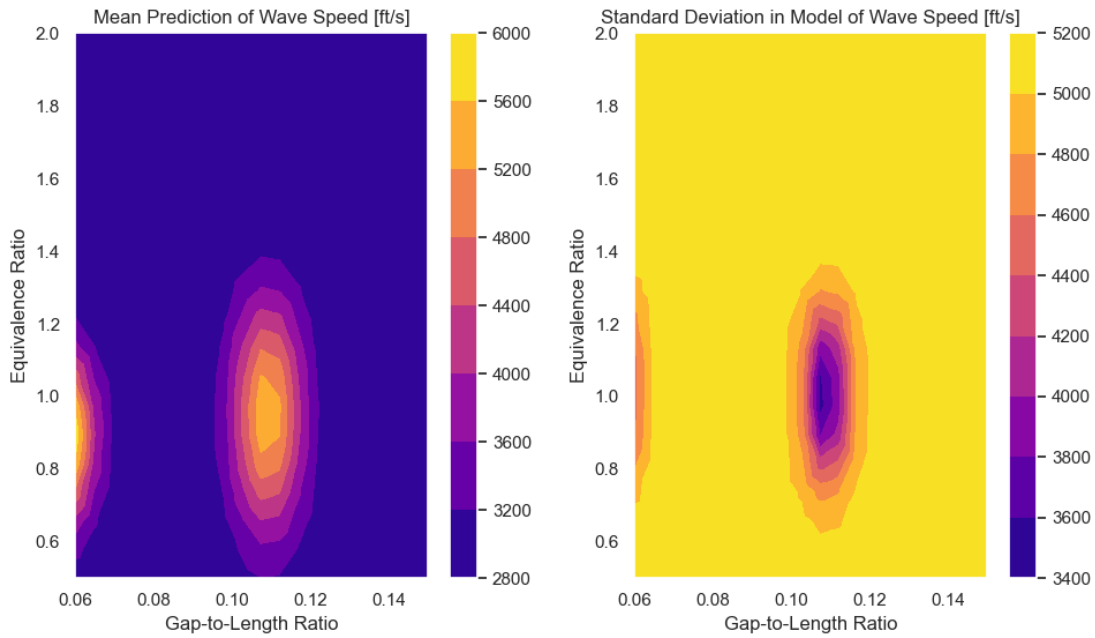
24

Fig. 29   Wave Speed Prediction for Constant $\dot{m}_T$
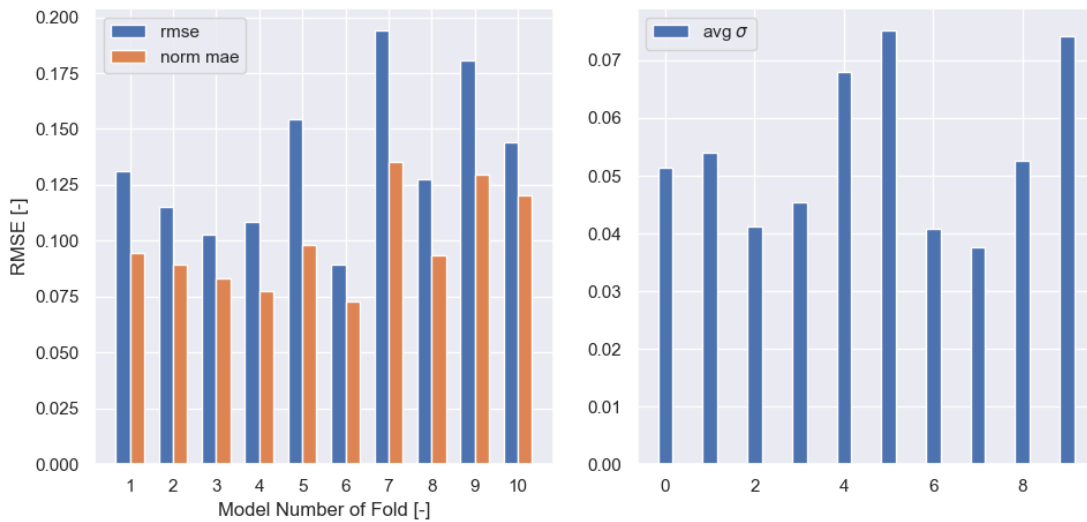
Fig. 30   N-Fold Error Analysis of Wave Speed Prediction
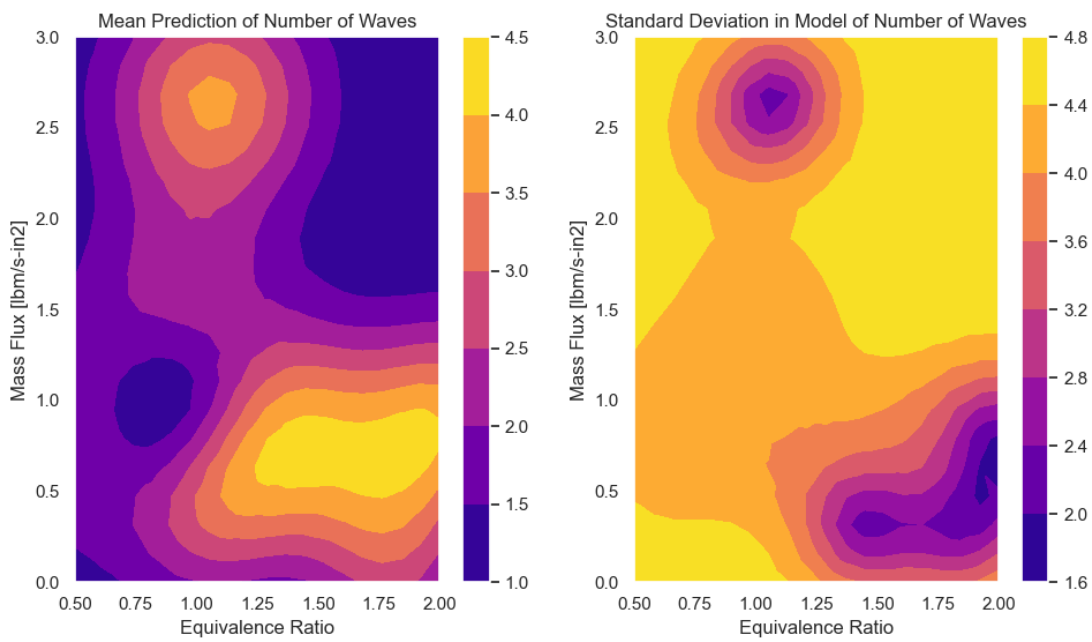
Fig. 31   Wave Number Prediction for Constant η
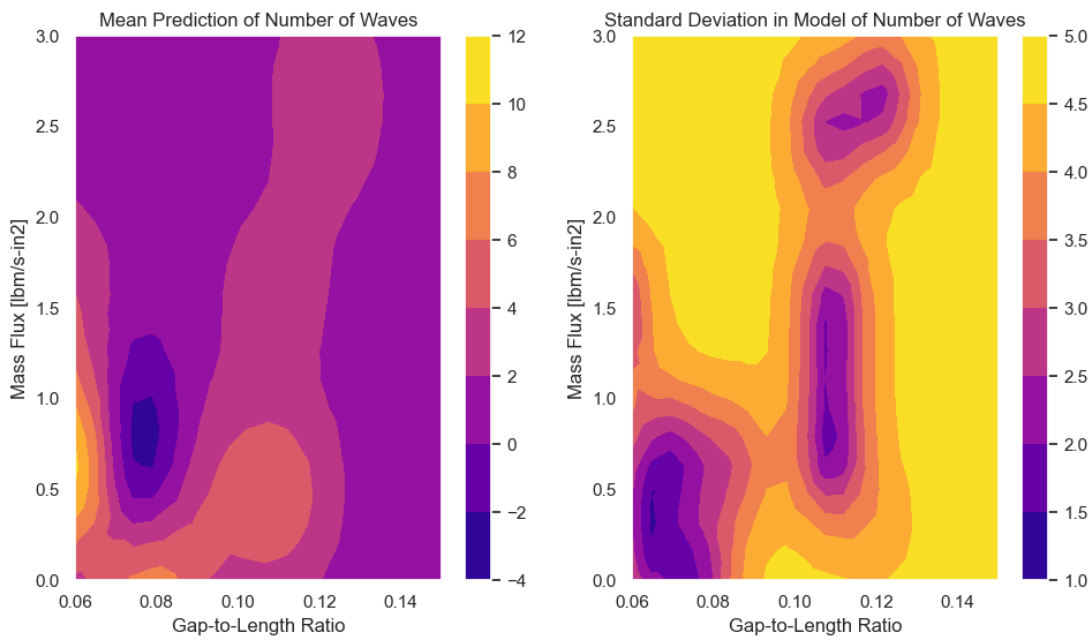
**Fig. 32   Wave Number Prediction for Constant ϕ**
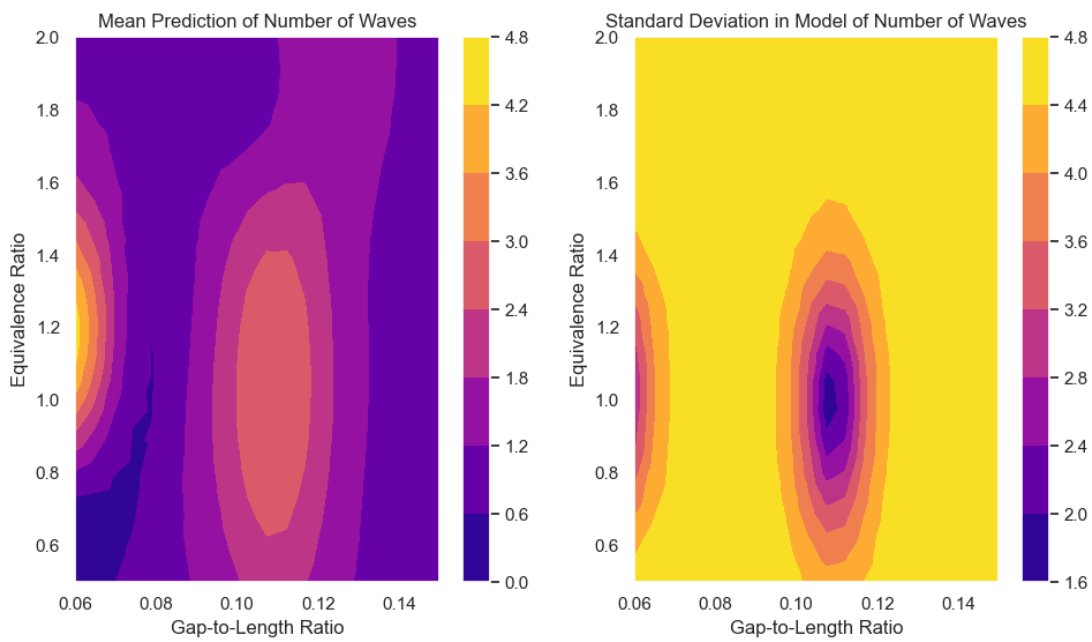
Fig. 33   Wave Number Prediction for Constant $\dot{m}_T$
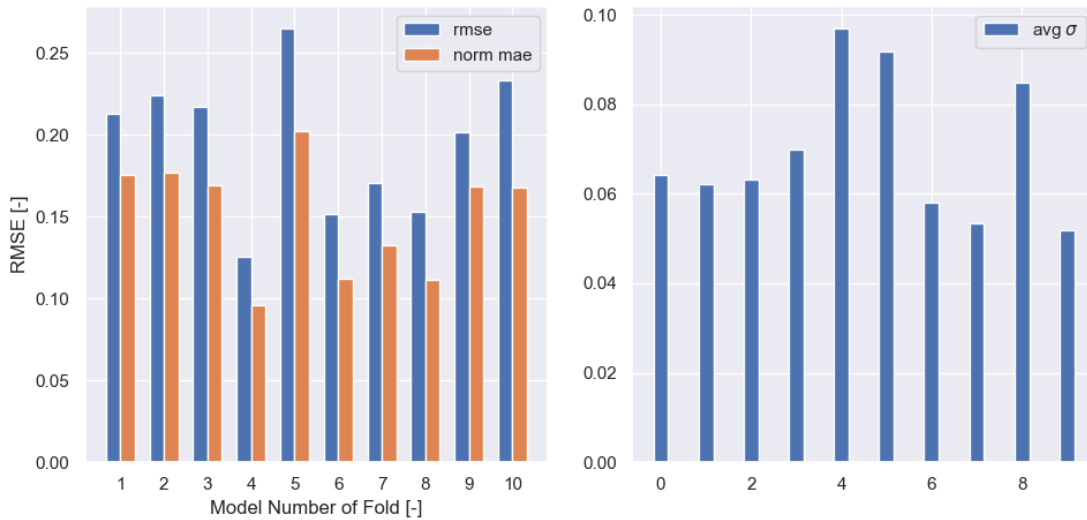
Fig. 34   N-Fold Error Analysis of Wave Number Prediction

Acknowledgments

References

[1] Johnson, K., Ferguson, D., and Nix, A. C., "Time Series Classification within a Rotating Detonation Engine through Deep Convolutional Neural Networks Applied to High-Pressure Data," *AIAA SciTech*, 2022.

[2] Mendible, A., Koch, J., Lange, H., Brunton, S. L., and Kutz, J. N., "Data-driven modeling of rotating detonation waves," *Physical Review Fluids*, Vol. 6, No. 5, 2021, p. 050507.

[3] Teasley, T. W., Williams, B., Larkey, A., Protz, C., and Gradl, P., "A Review Towards the Design Optimization of High-Performance Additively Manufactured Rotating Detonation Rocket Engines," *AIAA Propulsion and Energy*, 2021.

[4] Nejaamtheen, M. N., J, K., and J, C., *Detonation Control for Propulsion*, 1st ed., Springer International Publishing, 2018, Chap. Chapter 6: Review on Research Progresses in Rotating Detonation Engine.

[5] Zhou, R., Wu, D., and Wang, J., "Progress of Continuously Rotating Detonation Engines," *Chinese Journal of Aeronautics*, Vol. 29, No. 1, 2016, pp. 15–29.

[6] Young, M. T., Bechle, M. J., Sampson, P. D., Szpiro, A. A., Marshall, J. D., Sheppard, L., and Kaufman, J. D., "Satellite-Based NO2 and Model Validation in a National Prediction Model Based on Universal Kriging and Land-Use Regression," *Environmental Science & Technology*, Vol. 50, No. 7, 2016, pp. 3686–3694.

[7] Legleiter, C. J., and Kyriakidis, P. C., "Spatial Prediction of River Channel Topography by Kriging," *Earth Surface Processes and Landforms*, Vol. 33, No. 6, 2007, pp. 841–867.

[8] Jeong, S., Minemura, Y., and Obayashi, S., "Optimization of Combustor Chamber for Diesel Engine Using Kriging Model," *Journal of Fluid Science and Technology*, Vol. 1, No. 2, 2006, pp. 138–146.

[9] Unruh, E. C., "Development and Testing of a Rotating Detonation Rocket Engine with a Racetrack Combustor and Shear-Coaxial Injectors," , 2021.

[10] Teasley, T., Fedotowsky, T., Gradl, P., Austin, B., and Heister, S., "Current State of NASA Continuously Rotating Detonation Cycle Engine Development," *AIAA SciTech*, 2023.

[11] Goto, K., Nishimura, J., Kawasaki, A., Matsuoka, K., Kasahara, J., Matsuo, A., Funaki, I., Nakata, D., Uchiumi, M., and Higashino, K., "Propulsive Performance and Heating Environment of Rotating Detonation Engine with Various Nozzles," *AIAA Journal of Propulsion and Power*, Vol. 35, No. 1, 2019, pp. 213–223.

[12] Anderson, W. S., Heister, S. D., Kan, B., and Hartsfield, C., "Experimental Study of a Hypergolically Ignited Liquid Bi-Propellant Rotating Detonation Rocket Engine," *AIAA Journal of Propulsion and Power*, Vol. 36, No. 6, 2020.

[13] Bigler, B. R., Bennewitz, J. W., Danczyk, S. A., and Hargus, W. A., "Rotating Detonation Rocket Engine Operability Under Varied Pressure Drop Injection," *AIAA Journal of Spacecraft and Rockets*, Vol. 58, No. 2, 2021, pp. 316–325.

[14] Stechmann, D. P., "Experimental Study of High-Pressure Rotating Detonation Combustion in Rocket Environments," Ph.D. thesis, Purdue University, 2017.

[15] Krige, D. G., "A Statistical Approach to Some Basic Mine Valuation Problems on the Witwatersrand," *Journal of the Southern African Institute of Mining and Metallurgy*, Vol. 52, No. 6, 1951, pp. 119–139.

[16] Duvenaud, D. K., "Automatic Model Construction with Gaussian Processes," Ph.D. thesis, University of Cambridge, 2014.

[17] Rasmussen, C. E., and I, W. C. K., *Gaussian Processes for Machine Learning*, MIT Press, 2008.

[18] Wang, Z., Wang, K., Li, Q., Zhu, Y., Zhao, M., and Fan, W., "Effects of the Combustor Width on Propagation Characteristics of Rotating Detonation Waves," *Aerospace Science and Technology*, Vol. 105, 2020.

[19] Burr, J. R., and Paulson, E. J., "Thermodynamic Performance Results for Rotating Detonation Rocket Engine with Distributed Heat Additon using Cantera," *AIAA Propulsion and Energy Forum*, 2021.

[20] Russo, R. M., King, P. I., Shauer, F. R., and Thomas, L. M., "Characterization of Pressure Rise Across a Continuous Detonation Engine," *AIAA/ASME/SAI/ASEE Joint Propulsion Conference*, 2011.

[21] Luan, Z., Huang, Y., Gao, S., and You, Y., "Formation of Multiple Detonation Waves in Rotating Detonation Engines with Inhomogeneous Methane/Oxygen Mixtures Under Different Equivalence Ratios," *Combustion and Flame*, Vol. 241, 2022, p. 112091.

[22] Anand, V., and Gutmark, E., "Rotating Detonation Combustors and Their Similarities to Rocket Instabilities," *Progress in Energy and Combustion Science*, Vol. 73, 2019, pp. 182–234.

[23] Hunter, J. D., "Matplotlib: A 2D graphics environment," *Computing in Science & Engineering*, Vol. 9, No. 3, 2007, pp. 90–95. https://doi.org/10.1109/MCSE.2007.55.

[24] Harris, C. R., Millman, K. J., van der Walt, S. J., Gommers, R., Virtanen, P., Cournapeau, D., Wieser, E., Taylor, J., Berg, S., Smith, N. J., Kern, R., Picus, M., Hoyer, S., van Kerkwijk, M. H., Brett, M., Haldane, A., del Río, J. F., Wiebe, M., Peterson, P., Gérard-Marchant, P., Sheppard, K., Reddy, T., Weckesser, W., Abbasi, H., Gohlke, C., and Oliphant, T. E., "Array programming with NumPy," *Nature*, Vol. 585, No. 7825, 2020, pp. 357–362. https://doi.org/10.1038/s41586-020-2649-2, URL https://doi.org/10.1038/s41586-020-2649-2.

[25] pandas development team, T., "pandas-dev/pandas: Pandas," , Feb. 2020. https://doi.org/10.5281/zenodo.3509134, URL https://doi.org/10.5281/zenodo.3509134.

[26] Pedregosa, F., Varoquaux, G., Gramfort, A., Michel, V., Thirion, B., Grisel, O., Blondel, M., Prettenhofer, P., Weiss, R., Dubourg, V., Vanderplas, J., Passos, A., Cournapeau, D., Brucher, M., Perrot, M., and Duchesnay, E., "Scikit-learn: Machine Learning in Python," *Journal of Machine Learning Research*, Vol. 12, 2011, pp. 2825–2830.

[27] Waskom, M. L., "seaborn: statistical data visualization," *Journal of Open Source Software*, Vol. 6, No. 60, 2021, p. 3021. https://doi.org/10.21105/joss.03021, URL https://doi.org/10.21105/joss.03021.